

**APPLICATION OF NODAL INTEGRAL METHOD FOR
CONVECTION-DIFFUSION PHYSICS AND NAVIER-STOKES
EQUATIONS**

**THESIS SUBMITTED IN PARTIAL FULFILLMENT OF REQUIREMENTS FOR
THE DEGREE OF**

**MASTER OF ENGINEERING
IN THERMAL ENGINEERING**

BY

**YUVRAJ SINGH
REGISTRATION NO.: 801783018**

**UNDER THE SUPERVISION OF
DR. NEERAJ KUMAR
(ASSISTANT PROFESSOR)**



**MECHANICAL ENGINEERING DEPARTMENT
THAPAR INSTITUTE OF ENGINEERING AND TECHNOLOGY, PATIALA-147004,
PUNJAB, INDIA**

CERTIFICATE

I hereby declare that the dissertation entitled "**APPLICATION OF NODAL INTEGRAL METHOD FOR CONVECTION-DIFFUSION PHYSICS AND NAVIER-STOKES EQUATIONS**" is an authentic record of my work carried out as requirements for the award of the degree of **Master of Engineering in Thermal Engineering at Thapar Institute of Engineering and Technology, Patiala** under the supervision of **Dr. Neeraj Kumar (Assistant Professor, Mechanical Engineering Department)**. No part of the matter embodied in this report has been submitted to any other university or institute for the award of any degree.

Date: 22-July-2019


Yuvraj Singh

Roll No.801783018

Thapar Institute of Engineering and Technology, Patiala

It is certified that the above statement made by the student is correct to the best of my knowledge and belief.



Dr. Neeraj Kumar

Assistant Professor

Mechanical Engineering Department

Thapar Institute of Engineering and Technology, Patiala

ABSTRACT

Generic nodal integral method (NIM) based scheme is being utilized to solve the diffusion, convection-diffusion problems and navier-stokes equations in regular rectangle cartesian geometry. The problems taken into account in present work are 2D steady state diffusion with heat source, 1D steady state diffusion, 2D steady state convection-diffusion with heat source and flow in lid driven cavity with square obstacle at center. Numerical results for FDM and NIM are compared, with respect to analytical solution for diffusion and convection-diffusion problems. Different respective grid sizes have been used to capture problem flow domain for diffusion, convection-diffusion and lid driven cavity. The flow in lid driven cavity with square obstacle at center has been modelled successfully using discretized navier-stokes equations utilizing NIM. In case of diffusion and convection dominant diffusion, the NIM scheme yields far better results as compared to FDM for any given grid size and takes less computational time as contrasted with latter. For coarser meshes specifically, for most of the defined cases, the NIM converges to very low errors in comparison to FDM. i.e. approximately ten to hundred times less than latter. Due to this reason, in the present work, the NIM modelled discretized navier stokes equations has been used effectively to capture the flow profiles efficiently for lid driven cavity at any grid size, coarser or finer, for high or low reynold numbers ranging from 100 to 1000.

ACKNOWLEDGEMENTS

I would like to express my special thanks and sense of gratitude to my supervisor, Dr. Neeraj Kumar for the guidance. I have been extremely lucky to have a supervisor who helped me in my work and I came to know about so many new things. He provided me the technical support, facilities and skills that really helped me during the work. He cared so much about my work over the year.

Furthermore, I would like to express my sincere gratitude to the Mechanical Engineering Department, Thapar Institute of Engineering and Technology for the technical support. Further, I would like to thank specially my lab. members Amritpal Singh, Sandeep Nain and Gurmeet Singh for their technical and moral support. Finally, I would like to express my sincerest sense of gratitude to my family for their support and love for me, without which this work could not have been possible.

TABLE OF CONTENTS

	Page No.
Certificate	i
Abstract	ii
Acknowledgements	iii
Table of Contents	iv
List of Figures	v
List of Tables	vii
Nomenclature	viii
Abbreviations	ix
CHAPTER 1 INTRODUCTION	1
1.1 Motivation	1
1.2 Thesis Outline	3
CHAPTER 2 LITERATURE REVIEW	4
2.1 Introduction	4
2.2 Notable work	5
2.3 Gaps identified	11
2.4 Thesis objectives	12
CHAPTER 3 MATHEMATICAL FORMULATION	13
3.1 Basic methodology	13
3.2 Discretized steady state 2D equation with heat source	17
3.3 Discretized 1D convection-diffusion equation	18
3.4 Discretized steady state 2D convection-diffusion equation with heat source	18
3.5 Discretized Navier Stokes Equations	19
CHAPTER 4 NUMERICAL RESULTS AND DISCUSSIONS	22
4.1 Steady state 2D diffusion	22
4.2 1D convection-diffusion	23
4.3 Steady state 2D convection diffusion	24
4.4 Lid driven cavity with square shaped obstacle at center	26
CHAPTER 5 CONCLUSIONS AND SCOPE FOR FUTURE WORK	39
5.1 Conclusions	39
5.2 Scope for future work	39
REFERENCES	42
APPENDIX	45

LIST OF FIGURES

Figure 1. 1 : Flowchart of NIM methodology.....	2
Figure 3. 1 : Schematic of the global (x, y) space, and its division into computational elements.....	14
Figure 3. 2 : Discretization of spatial domain into nodes	14
Figure 3. 3 : Local coordinate system with node (i, j)	14
Figure 3. 4 : Transverse averaged quantities on the surface	15
Figure 3. 5 : Transverse averaged velocity components on x and y surfaces respectively.....	20
Figure 4. 1 : Implemented boundary conditions for given problem domain	22
Figure 4. 2 : Implemented boundary conditions for given problem domain	25
Figure 4. 3 : Implemented boundary conditions at lid and blockage surface	26
Figure 4. 4 : Plot showing comparison in variation of transverse averaged velocity component (v^x) distribution in x-direction at blockage size (0.1 of the total length of cavity) and $Re=1000$	27
Figure 4. 5 : Plot showing comparison in variation of transverse averaged velocity component (u^y) distribution in y-direction at blockage size (0.1 of the total length of cavity) and $Re=1000$	28
Figure 4. 6 : Plot showing comparison in variation of transverse averaged velocity component (v^x) distribution in x-direction at blockage size (0.1 of the total length of cavity) and $Re=400$	29
Figure 4. 7 : Plot showing comparison in variation of transverse averaged velocity component (u^y) distribution in y-direction at blockage size (0.1 of the total length of cavity) and $Re=400$	29

Figure 4. 8 : Plot showing comparison in variation of transverse averaged velocity component (v^x) distribution in x-direction at blockage size (0.1 of the total length of cavity) and $Re=100$ 31

Figure 4. 9 : Plot showing comparison in variation of transverse averaged velocity component (u^y) distribution in y-direction at blockage size (0.1 of the total length of cavity) and $Re=100$ 31

Figure 4. 10 : Plot showing comparison in variation of transverse averaged velocity component (v^x) distribution in x-direction at blockage size (0.2 of the total length of cavity) and $Re=1000$ 32

Figure 4. 11 : Plot showing comparison in variation of transverse averaged velocity component (u^y) distribution in y-direction at blockage size (0.2 of the total length of cavity) and $Re=1000$ 32

Figure 4. 12 : Plot showing comparison in variation of transverse averaged velocity component (v^x) distribution in x-direction at blockage size (0.2 of the total length of cavity) and $Re=400$ 33

Figure 4. 13 : Plot showing comparison in variation of transverse averaged velocity component (u^y) distribution in y-direction at blockage size (0.2 of the total length of cavity) and $Re=400$ 33

Figure 4. 14 : Plot showing comparison in variation of transverse averaged velocity component (v^x) distribution in x-direction at blockage size (0.2 of the total length of cavity) and $Re=100$ 34

Figure 4. 15 : Plot showing comparison in variation of transverse averaged velocity component (u^y) distribution in y-direction at blockage size (0.2 of the total length of cavity) and $Re=100$ 34

Figure 4. 16 : Stream function defined at respective nodes in problem domain35

Figure 4. 17 : Stream trajectories of transverse averaged flow component u^y for problem domain (50x50 grid size) at blockage size (0.1 of total length of cavity) and $Re=1000$ 36

Figure 4. 18 : Stream trajectories of transverse averaged flow component u^y for problem domain
(50x50 grid size) at blockage size (0.1 of total length of cavity) at $Re=1000$37

Figure 4. 19 : Stream trajectories of transverse averaged flow component u^y for problem domain
(50x50 grid size) at blockage size (0.1 of total length of cavity) and $Re=100$37

Figure 4. 20 : Stream trajectories of transverse averaged flow component u^y for problem domain
(50x50 grid size) at blockage size (0.2 of total length of cavity) and $Re=1000$38

Figure 4. 21 : Stream trajectories of transverse averaged flow component u^y for problem domain
(50x50 grid size) at blockage size (0.2 of total length of cavity) and $Re=400$38

Figure 4. 22 : Stream trajectories of transverse averaged flow component u^y for problem domain
(50x50 grid size) at blockage size (0.2 of total length of cavity) and $Re=100$39

LIST OF TABLES

Table 4. 1 : Comparison between relative error for solutions obtained utilizing FDM and NIM with respect to analytical solution.....	23
Table 4. 2 : Comparison between relative error for solutions obtained utilizing FDM and NIM with respect to analytical solution.....	23
Table 4. 3 : Comparison between relative error for solutions obtained utilizing FDM and NIM with respect to analytical solution.....	24
Table 4. 4 : Comparison between relative error for solutions obtained utilizing FDM and NIM with respect to analytical solution.....	26

NOMENCLATURE

α	Thermal Diffusivity
pev	Peclet number
Re	Reynold number
Pr	Prandtl number
u	Mean flow velocity
q	Heat flux
ν	Viscosity of fluid
\vec{w}	Velocity vector
i, j	Subscripts in x and y direction respectively, defining nodal index

ABBREVIATIONS

CDE	:	Convection Diffusion Equation.
FDM	:	Finite Difference Method.
FVM	:	Finite Volume Method.
JFKM	:	Jacobian Free Newton Krylov Method.
MNIM	:	Modified Nodal Integral Method.
MPI	:	Message Passing Interface.
NGFM	:	Nodal Green Function Method.
NI-FAM	:	Nodal Integral-Finite Analytic Method.
NI-FEM	:	Nodal Integral-Finite Element Method.
NIM	:	Nodal Integral Method.
ODE	:	Ordinary Differential Equation.
PDE	:	Partial Differential Equation.
QUICK	:	Quadratic Upstream Interpolations for Convective Kinetics.
SIMPLE	:	Semi Implicit Method based Pressure Linked Equations.
TIP	:	Transverse Integration Procedure.

CHAPTER 1

INTRODUCTION

1.1. MOTIVATION

Discretization of neutron diffusion issues utilizing conventional limited contrast strategies requires very fine mesh or larger number of discrete nodal points to precisely capture the spatial variety of the neutron motion.

The computational cost related with these conventional methods spurred the early improvement of less thorough, yet more computationally proficient systems arranged towards the assurance of the motion averaging each dependent variable over the nodal surface.

This class of techniques hence ended up known as nodal strategies, and the FLARE model 3 created in 1964 is illustrative of the original of these plans [1].

The distinctive component of nodal essential strategy is transverse coordination procedure of administering PDE in each sub-space called domain of the issue area. The distinctive component of nodal basic technique is transverse combination procedure of overseeing PDE in each sub-area called hub of the issue space. This transverse incorporation over the hub measurements of everything except one free factor diminishes every one of the PDE to an ODE [1-8]. After rehashed coordination m sets of ODEs could be gotten for a PDE, where m is the quantity of free factors. The arrangement of ODEs can normally be understood more effectively than the first PDEs.

Since shut structure accurate arrangements of the arrangement of ODEs are, by and large, impractical, this progression is just performed incompletely: the straight piece of the ODEs is comprehended while non-direct terms are treated as inhomogeneous terms (generally called the pseudo-source term) with specific arrangements worked out for them. The way that the piece of ODEs (the direct part) is unraveled precisely guarantees that the basic arrangements are significant to the issue, prompting straight, quadratic, trigonometric, or exponential (hyperbolic) arrangements as managed by a bit of the administering conditions. This methodology of illuminating piece of the condition diagnostically enables the NIM to yield a fairly precise arrangement even with just a couple of terms in extension.

In spite of the fact that the NIM is very exact, its materialness is confined to a physical area fitted into the Cartesian arrange framework. This limitation is because of the coefficients in discretized

coupling conditions for transverse averaged factors. This impediment is facilitated somewhat by coupling a NIM-based plan with limited component or limited diagnostic plans to produce a half breed conspire. Toreja et al. [7] and Gu et al. [16] utilized such cross breed plans for liquid stream and neutron diffusion conditions, individually. In another methodology, logarithmic change has been utilized by Nezami et al. [9] to delineate formed quadrilateral components to rectangular components. Bi-straight Lagrange insertion capacities have been utilized to delineate molded quadrilaterals to square unit components, which are routinely utilized in FEM-based plans [7]. Utilizing this methodology, Nezami et al. [9] created and illuminated the convection-diffusion condition.

The NIM scheme in present work is developed in following order:

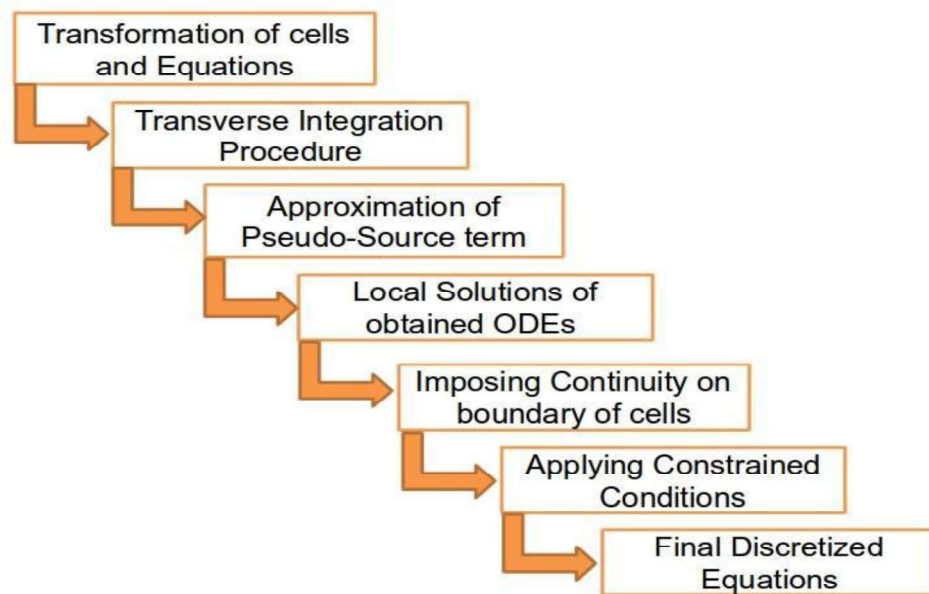


Figure 1. 1 : Flowchart of NIM methodology

1.2 THESIS OUTLINE

Chapter 1 gives the motivation behind the present thesis work. It includes reasons, process and need of the present work that is applying NIM successfully over coarse grid surfaces as compared to method like FDM which proves to be less efficient in this regard. Chapter 2 is the review of the literature which I have gone through during my thesis work. Gaps identified and thesis objectives are also being noted down in this chapter. This process has given me diverse perspectives, data and much useful information related to my present work. Mathematical formulation has been presented in Chapter 3. This chapter gives the methodology, formulation and assumptions that were used to model the NIM scheme. It describes the mathematical procedure by which NIM scheme can be formulated. Chapter 4 gives the results and outcomes of the numerical simulation of various diffusion, convection-diffusion problems and lid driven cavity problem with obstacle at center. The developed NIM scheme is tested and verified on each problem taken into account in present work on different grid sizes. The results generated for diffusion and convection-diffusion problems utilizing NIM scheme, are compared with FDM and validated with respect to analytical solution. Chapter 5 details the conclusion of the present work and scope for future work.

CHAPTER 2

LITERATURE REVIEW

2.1 INTRODUCTION

The convection-diffusion equation administers the transport of scalar factors by advection or potentially diffusion transport. This equation is additionally the least complex model equation for demonstrating the greater part of the transport phenomena in fluid flow and heat transfer issues. In spite of the fact that these administering differential (convection-diffusion, diffusion) equations are linear, they are agreeable to scientific arrangements just in limited geometries. Indeed, the numerical arrangements are inclined to numerical unsteadiness because of the non-linear irksome convective term in the convection-diffusion equation. Since these equations are building hinders for administering differential equations for complex stream, i.e., Navier-Stokes equations, various numerical plans have been created and utilized throughout the most recent couple of decades to illuminate the convection-diffusion equation in and around complex geometries [1–5] utilizing limited distinction strategies (FDM), finite volume techniques (FVMs), and limited component techniques (FEMs).

The nodal indispensable techniques, otherwise called cell-logical strategies, have been created and connected to understand halfway differential conditions in different parts of science and engineering. These strategies are outstanding for giving very exact arrangements on a sensibly coarse work contrasted with ordinary numerical systems [6–11]. The purpose for the high exactness is the diagnostic pre-handling associated with the discretization procedure [8–10]. This logical pre-preparing establishes the transverse reconciliation process (TIP), which is utilized to create cell (neighborhood) scientific arrangements of transverse arrived at the midpoint of field factors over the discretized area. Another strategy, called the nodal warmth balance necessary technique (HBIM), additionally takes a shot at an estimated arrangement work over every subdivision (hub) of the issue area, this surmised profile in the HBIM inside the neighborhood space is discretionary in nature and its relevance is constrained to a couple of issues, for example, the Stefan issue [12].

2.2 NOTABLE WORK

Nodal integral technique is created based on transverse averaging which is a novel system of nodal strategies. Numerous analysts adjusted the nodal techniques, coming about different type of these strategies as changed NGFM, NIM, MNIM, NIFEM, NIFAM and numerous different strategies are developed from these nodal techniques. Their works and discoveries have been quickly condensed beneath:

1. **Fischer and Finnemann** [5] have built up a logical nodal strategy, NIM, to explain the three dimensional, coupled neutron diffusion equations. Transverse averaging of spillage shapes was done as far as parabolas which was the main estimation in this methodology. To decide the coefficients of parabola, two distinct strategies were utilized in this article. This technique, NIM, was tried and confirmed against seat mark arrangements of neutron diffusion condition. Nodal integral strategy (NIM) yields another different solver, other than NEM, which is notable in nuclear industry. Both the solvers NIM and NEM were utilized in same emphasis way with the goal that they can without much of a stretch be traded in reactor center test system. This subsequent a differing solver for on location use in plant control frameworks.
2. **Lawrence and Dorning** [17], have built up a nodal strategy to explain the multidimensional neutron diffusion equation. This technique depended on the linear type of nodal balance equation. These nodal balance equations were characterized as far as normal partial currents over the surface of node. A lot of coupled 1-D integral equations, which were characterised over the neighborhood discrete sub-areas, was produced utilizing Green's function capacities. Transverse coordinating method, diminished the multidimensional neutron diffusion equation to the coupled arrangement of one-dimensional common differential equations which were gotten over the transverse headings. Coming about, integral equations were accurate arrangements characterized over a nodal cell. Moreover, these integral equations were approximated with weighted residuals inside each nodal cell. This estimate prompts grid equations, which were explained with linear nodal balance equation. The said nodal balance equations give extra connection between the motion inside the node and interface of partial currents. The created strategy was tried with a four-bench fluid metal quick raiser reactor issues and furthermore with 2D and 3D light water reactor benchmark issues. The got outcomes demonstrates the capacity of nodal techniques which can produce extremely exact outcomes with huge little computation time in contrast with the standard limited distinction strategies (FDM).

3. **Azmy and Dorning** [18], For steady state stream issues (Navier-Stokes), Nodal integral technique (NIM) was created. Be that as it may, the NIM strategy was as yet dependent on the conventional transverse averaging technique (TIP), the strategy was unique in relation to the past nodal green capacity technique (NGFM) due to a smaller number of unknowns for a dependent variable. Consequently because of absence of multifaceted nature, NIM was much effectively utilized in complex issues. The created scheme was tried with different liquid stream (Flow between parallel plates and Lid driven pit) and warmth move (Boussinesq guess for regular convection) issues. On check of NIM scheme with benchmark arrangements, it was inferred that the scheme is very exact on moderately coarse networks.
4. **Horek and Dorning** [19] have built up a proficient nodal technique utilizing transverse coordination strategy for incompressible laminar flow physics. Local Green's tensors were additionally presented in transverse averaged Navier-Stokes equations and continuity equations. This scheme was tried with different 2D experiments including inlet flow, completely created flow, adjusted driven cavity issues with inlet and outlet segments. The nodal Green's tensor technique demonstrated high exactness, which lead to a proficient computational strategy with very coarse matrix sizes. In any case, the fundamental disservice of this approach is that, it delivers increasingly unknowns for a dependent variable. In this way multifaceted nature of this strategy is as yet a drawback in contrast with NIM scheme.
5. **Azmy, Y.Y.** [3] have additionally changed the current nodal techniques and built up a nodal integral strategy (NIM) for illuminating the neutron diffusion equation in cylindrical geometry. Since the customary nodal strategies were confined to rectangular computational areas, this change increments the appropriateness of nodal technique over complex curvilinear geometry. The created numerical scheme was tried with two issues which were gotten by Exterminator-2 code. The outcomes demonstrate that nodal integral technique is computationally proficient and requires less CPU times in contrast with the typical limited distinction strategies (FDM) and limited component techniques (FEM). Anyway, the created nodal scheme and set of last discrete equations are more muddled than the other customary partners.
6. **Hennart, J.P.** [20] In this article, premise numerical investigation has been done of nodal expository strategies, which were initially produced for nuclear reactor issues and further reached out for numerical arrangement of PDEs. The discretization of issue area was finished utilizing the standard nodal cells. In this article transverse integration for an independent variable was utilized for parent PDE which prompts a lot of 1D-ODEs for that independent variable. These ODEs were

unraveled systematically, utilizing specific integral technique just as different essentials. After the exhaustive examination of existing scientific techniques, an all-encompassing explanatory strategy was proposed. The ends were made in the interest of super assembly results with individual specific scheme.

7. **Wilson et al.** [21] have created two new nodal integral strategies: one, lower order and other higher order to fathom the time-dependent, incompressible normal convection issue. Both of the strategies were higher level exact even with huge network estimate and can deliver results independent of Courant condition. The outcomes were created for various experiments: one, twofold looking, to confirm the precision in space time and other, bifurcation searches and security of flow locals. These experiments demonstrated the capacity of NIM scheme to copy the characteristic wonders without bifurcation focuses, defining moments and misleading arrangements, contrasted with the benchmark issues. The created schemes were additionally used to inspect the critical aspect proportion at which the elective stable arrangements can be acquired from a no-flow condition.
8. **Michael et al.** [22] Third order nodal integral strategy was created in this article. The recently announced second order nodal strategy was evaluated in this article for improvement and correlation of third order NIM. The linear piece of pseudo-source terms which show up in transversely incorporated equations was approximated by presenting upwind estimation. This estimate was presented in NIM scheme. In the conventional NIM system, extra equations are required for closer type of scheme plan. This convention was hindered by presenting upwind estimation in NIM scheme. The second-order nodal scheme and the third order NIM which has two renditions: one, full third order nodal technique and the other, which utilized second order equations close to the limits were contrasted with late created best in class strategy and other conventional strategies. The relative examination demonstrated that among the concentrated five techniques, second-order NIM scheme has most elevated computational effectiveness with 1% error.
9. **Rizwan Uddin** [22] NIM was produced for one dimensional advection-diffusion equation. This NIM scheme depended on the nodal approach and results second order numerical scheme for both reality factors. This scheme demonstrated natural upwinding and can be additionally stretched out to multidimensional issues. Coupling of nodal schemes with inside reproduction of the arrangement results an amazing numerical scheme that can resolve the locales with sharp inclinations even with generally coarse framework. Three experiments of convection-diffusion equation were explained utilizing the created NIM scheme to exhibit the exactness of scheme.

10. **Rizwan Uddin** [23] have adjusted the current nodal integral technique to illuminate the PDEs. In this change, nonlinear terms or supposed pseudo-source terms were treated by approximating the piece of non-linear terms of discrete field factors rather than entire pseudo-source terms. Remaining part or complete pseudo-source terms of transverse-incorporated equations were kept left-hand side and to be settled analytically. This adjustment diminished the intricacy of strategy and furthermore give conclusion type of definition process. This changed NIM was tried with Burger equation which lead to exponential variety of field variable inside the nodal cell. Coming about scheme for Burger equation demonstrated natural upwinding because of exponential terms. Transverse integration strategy (TIP) for an independent variable decrease a PDE as an element of that independent variable, arrived at the midpoint of every other way. This TIP enables NIM to get precise outcomes even on coarse matrix. The acquired numerical outcome were contrasted with the aftereffects of other contemporary techniques. The similar investigation demonstrated that the grew new strategy was practically identical and, in some cases, produces better outcomes than the right now utilized schemes. These schemes can be additionally reached out to multidimensional and time-dependent issues.
11. **Toreja and Rizwan** [7] have created two cross breed numerical schemes. NI-FAM was created utilizing nodal-integral strategy with limited explanatory technique (FAM) and NI-FEM was created utilizing NIM with limited component strategy (FEM). Both the schemes were created to settle two-dimensional, time-dependent just as relentless state convection diffusion equation (CDE). The computational space was discretized utilizing rectangular just as triangular nodes. Rectangular components were utilized for inside of space just as vertical and flat limits. Notwithstanding, the limits which were not either vertical or level were discretized utilizing triangular components. In time-dependent issue, the triangular and rectangular component moved toward becoming space-time wedge and parallelepiped molded nodes, individually. At the interface of nearby rectangular/parallelepiped nodal cell, distinction scheme was produced for arrived at the midpoint of factors utilizing ordinary NIM. In NI-FEM preliminary capacity was utilized for triangular components. This preliminary capacity was made to fulfill advection-diffusion equation in integral sense and written regarding edge-found the middle value of centralization of three edges. In NI-FAM, limited scientific guess was utilized for portrayal of the focus over the wedge/triangular molded cells. This limited expository guess was made by fulfilling the scientific arrangement of one dimensional CDE. For both the half and half schemes, contrast schemes were created at the interfaces of triangular/wedge and rectangular/parallelepiped-formed

components by applying the coherence state of the transition crosswise over interface.

12. **Wang and Rizwan** [4], built up a novel numerical scheme for time-dependent, incompressible, Navier-Stokes equations coupled with pressure Poisson equations. TIP was connected to these PDEs and changed over them to transverse averaged ODEs. These ODEs were in terms of discrete factors pressure and averaged velocities. Besides, these ODEs were comprehended in terms of averaged factors and after that used to build up the distinction scheme. This semi-certain scheme was created for block like cells and has inalienable upwinding. The variety of transverse-averaged pressure was viewed as quadratic spatial way. Anyway, the variety of transverse averaged speed was the total of a linear term and an exponential term. Deferred coefficients were additionally used in this scheme which prompts one assessment for each time step. A few test issues were tried and the outcomes demonstrated the power of nodal scheme because of second order mistake. The scheme performed great and lead to little mistakes even with enormous lattice sizes.
13. **Nezami et al.** [9] right off the bat built up the Nodal integral techniques (NIMs) for self-assertive formed quadrilateral components which loosened up the geometry confinement of NIM schemes. These NIM based schemes were utilized to tackle the different overseeing equations of various territories of flow physics. These schemes are incredible numerical schemes which can explain the overseeing PDEs precisely even with very coarse network. Anyway, an extraordinary method of NIM schemes, transverse averaging strategy (TIP) confines NIM to understand these PDEs in block like cells which constrains its application in complex geometries. This confinement was backed out by Nezami et al. [8]. The discretization was finished utilizing self-assertive quadrilaterals which expanded the pertinence of NIM scheme in complex space. These self-assertive quadrilaterals were changed to unit square components by utilizing Lagrange bi-linear introduction work. The administering equations were additionally changed to these neighborhoods square computational area. Presently the changed PDEs were tackled utilizing conventional NIM. This scheme was tried with Poisson equation just as time-dependent advection-diffusion equations. The created results were checked with benchmark issues. The outcomes were very encouraging and demonstrated that mathematical change with NIM scheme holds its precision with coarse framework sizes.
14. **Huang and Rizwan**, [25], have additionally built up crafted by Nezami et al. [8] for time-dependent, incompressible Navier-Stokes equations. Altered NIM scheme was created to unravel the Navier-Stokes equations in self-assertive formed spaces. Again, the four noded components are utilized in discretization methodology. Mathematical change was utilized to change the self-

assertive quadrilateral components into discrete square cells. This arithmetical change was finished utilizing bi-linear Lagrange insertion work like the methodology of Nezami et al. [8]. Navier-Stokes equations just as pressure Poisson equation were likewise changed to the neighborhood arrange framework. Adjusted NIM scheme was utilized to unravel the two-dimensional shear-driven hole issue and the outcomes were contrasted and the explanatory arrangement. The outcomes were very encouraging and demonstrated that precision of changed NIM can be kept up utilizing non-rectangular components. These NIM scheme can be additionally stretched out for bended spaces.

15. **Kumar et al.** [12] built up a pressure adjustment put together calculation based with respect to NIM philosophy to understand the unfaltering state, 2-D incompressible Navier-Stokes equations. Partial differential equations of various zones of physics have been explained utilizing NIM schemes which show high precision in sensible coarse network in contrast with other ordinary schemes. Semi-Implicit Method for Pressure-Linked Equations (SIMPLE) like calculation was utilized in execution of the NIM scheme. In this calculation pressure and speed remedy are utilized as opposed to comprehending precise pressure Poisson equation. The created scheme is confirmed and tried against two test issues, normal convection of air in a square cavity and shear-driven depression. For both the experiments NIM schemes performs great and the produced outcomes are in great concurrence with benchmark arrangements even with very coarse matrix estimate.
16. **Kumar et al.** [13], built up a conventional numerical scheme dependent on the NIM approach to illuminate convection-diffusion equation in complex area. Two dimensional subjective molded linear quadrilateral components were utilized for discretization of issue do-fundamental. Every quadrilateral was mapped to unit square component utilizing isoparametric one-one onto mapping. This mapping was finished utilizing Lagrange bi-linear introduction work. Likewise, a novel numerical scheme was created for execution of Neumann and blended sort limit condition for discretionary molded limit. At the interface of two neighboring discrete components, continuity condition was expressly planned. Testing and confirmation of created scheme was likewise finished with expository arrangement of Convection-diffusion and Diffusion equation in slanted and bended geometry. The created numerical outcomes concurred genuinely well with diagnostic outcomes even with sensibly coarser frameworks. It was reasoned that NIM schemes have the ability to deliver exact outcomes with a lot of coarser networks even with curvilinear geometries.
17. **Kumar et al.** [14], built up a numeric scheme which is like the scheme for Convection-Diffusion equation. This scheme depended on Nodal Integral Method (NIM) and created for explaining

Navier-Stokes equations in self-assertive formed area. Pressure correction-based calculation are utilized for assembly condition and pressure Poisson equation are fathomed like the diffusion equation. This pressure Poisson equation supplanted the coherence condition and SIMPLE like calculation was utilized to guarantee the combination criteria. Two test issue, Shear-driven depression and buoyancy-driven flows were numerically explained for testing and check of NIM based scheme. The relative investigation was additionally done and the gotten outcomes were contrasted and fine work arrangement of past examinations utilizing FVM and comparative schemes. It was presumed that NIM based schemes for Navier-Stokes equations have the ability to create very precise outcomes even with very coarse and non-symmetrical lattices.

2.3 GAPS IDENTIFIED

1. Traditional numerical techniques require extremely fine networks to acquire the precise outcomes which prompts higher computational expenses. In this way a numerical technique is required which yield precise outcomes with coarse work.
2. Nodal integral strategy is a coarse network technique which satisfy the above prerequisite yet at the same time limited to customary computational space because of its extraordinary transverse integration system (TIP).
3. These nodal techniques were produced for unpredictable areas utilizing distinctive sort of components in discretization strategy of the perplexing and curvilinear spaces. NIM schemes still require fine networks to determine the bended geometry.
4. Although, the regular geometry restriction of NIM is eased out using linear quadrilateral elements but the curved boundaries still discretized using linear elements which is not a realistic approach.
5. Most scientists utilized linear guess in NIM system. This guess just works with linear components, so subsequent change is as yet required in NIM approximations for higher order components.
6. Currently created Neumann and blended sort of limit conditions are utilized for linear quadrilateral components even with bended limits which incorporate blunder in numerical arrangements. In this way legitimate usage of these sort of limit conditions are required.
7. Since, no work is accounted for in regards to the conduct of NIM scheme with one-sided and non-symmetrical lattices.

Along these lines, a careful report is required for utilizing this scheme in complex flow issues.

2.4 THESIS OBJECTIVES

1. To build up a conventional numerical scheme dependent on NIM system for diffusion, convection-diffusion and Navier-stokes equations utilizing both regular cartesian geometry.
2. To study comparison between FDM and NIM and validate the results with respect to analytical solution for various diffusion and convection-diffusion problems.
3. To model the flow in lid driven cavity with square solid blockage at center using discretized Navier-stokes equations utilizing NIM scheme.

CHAPTER 3

MATHEMATICAL FORMULATION

3.1 Basic Methodology

The governing equation of convection-diffusion phenomena is given as:

$$-\epsilon \nabla^2 u + \vec{w} \cdot \nabla u = f$$

where ϵ (represents thermal diffusivity or viscosity of fluid) > 0 . This condition emerges in various models of streams and other physical wonders. The obscure capacity u may speak to the grouping of a contamination being transported (or "convected") along a stream moving at speed \vec{w} and furthermore subject to diffusive impacts. Then again, it might speak to the temperature of a liquid moving along a warmed divider, or the grouping of electrons in models of semiconductor gadgets. This condition is additionally a central subproblem for models of incompressible stream, where u is a vector-esteemed capacity speaking to stream speed and ϵ is a viscosity parameter. Normally, dispersion is a less critical physical impact than convection: on a blustery day the smoke from a smokestack move toward the breeze and any spreading because of sub-atomic dispersion is little. This suggests, for most functional issues, $\epsilon \ll u$.

But to illustrate and formulate the method given in present work i.e. NIM (Nodal Integral Method), we have taken the example of most common steady state 2D diffusion case with heat source, whose governing equation is given as:

$$\frac{\partial^2 T}{\partial x^2} + \frac{\partial^2 T}{\partial y^2} + f(x, y) = 0 \quad (3.1)$$

where $f(x, y)$ is heat source term in given problem domain. The above equation is coordinated transversely for a hub over every each one of the autonomous factors (x, y) . Transverse coordination is implemented by operating, $\frac{1}{2a_{i,j}} \int_{-a_{i,j}}^{a_{i,j}} dx$ and $\frac{1}{2b_{i,j}} \int_{-b_{i,j}}^{b_{i,j}} dy$, where $a_{i,j}$ and $b_{i,j}$ are dimensions of node (i, j) in x and y direction respectively as shown in figure 3.1 and 3.3.

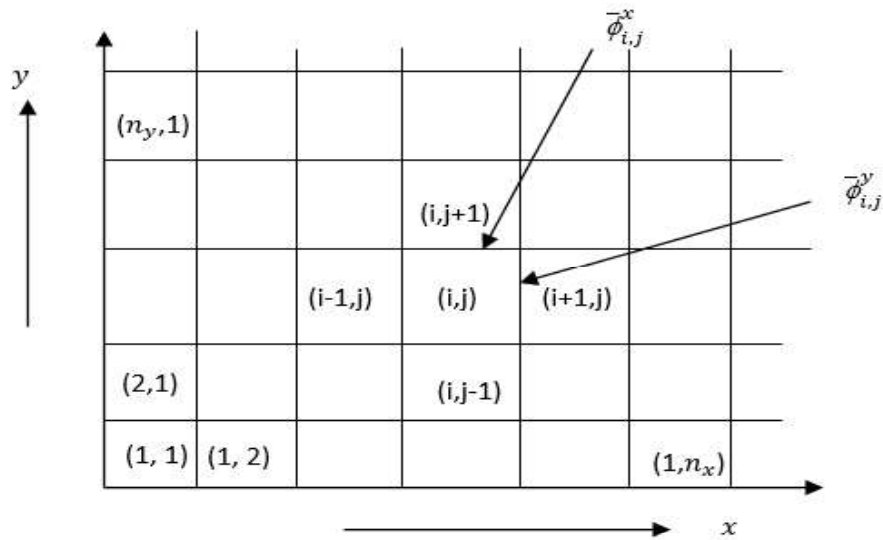


Figure 3. 1 : Schematic of the global (x, y) space, and its division into computational elements

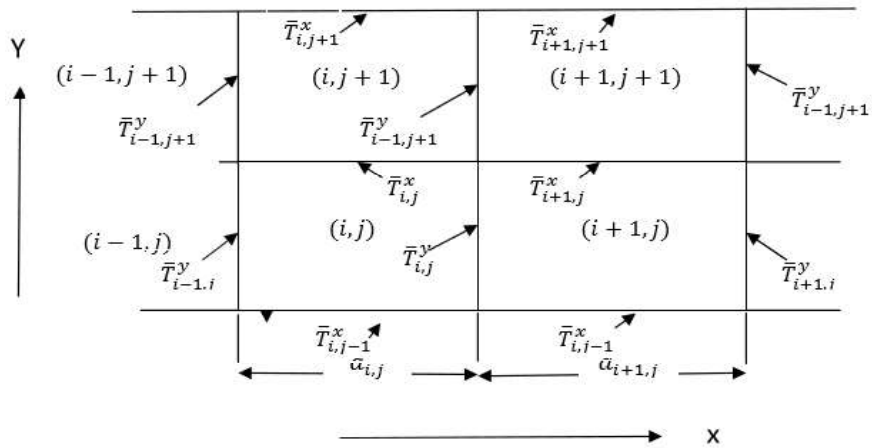


Figure 3. 2 : Discretization of spatial domain into nodes

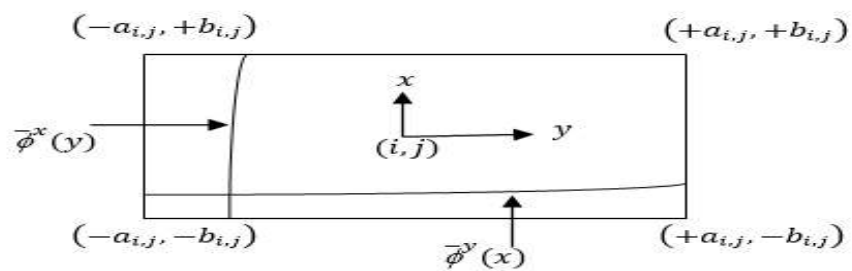


Figure 3. 3 : Local coordinate system with node (i, j)

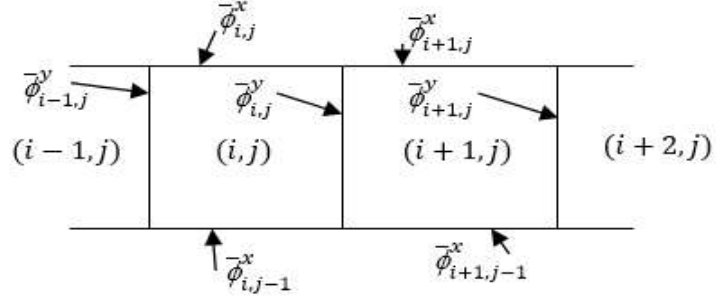


Figure 3. 4 : Transverse averaged quantities on the surface

After transverse combination over the spatial node and extending the source term by Legendre polynomial and truncating at zeroth dimension, the last two arrangement of conventional differential conditions:

$$\frac{d^2 \bar{T}^x}{dy} = \bar{S}_1^{xy} - \bar{f}_1^{xy} \quad (3.2)$$

$$\frac{d^2 \bar{T}^y}{dx} = \bar{S}_2^{yx} - \bar{f}_1^{yx} \quad (3.3)$$

\bar{T}^x and \bar{T}^y , are averaged temperatures in x and y direction respectively which are shown in fig. 3.2. \bar{S}_1^{xy} and \bar{S}_2^{yx} are pseudo source terms. Eq. (3.2) and Eq. (3.3) are integrated, the nodal boundary conditions are applied to evaluate the constants of integration and then applying the continuity condition at nodal interface for both in x and y direction gives three-point scheme in x and y directions respectively.

The coupling equation between two nodes is derived by applying continuity at interface between i^{th} and $(i + 1)^{\text{th}}$ spatial nodes as shown in fig.3.4.

$$\bar{T}_{i,j}^y(+a_{i,j}) = \bar{T}_{i+1,j}^y(-a_{i+1,j})$$

$$\frac{d\bar{T}_{i,j}^y(+a_{i,j})}{dx} = \frac{d\bar{T}_{i+1,j}^y(+a_{i+1,j})}{dx}$$

The three-point scheme in y direction that relate j^{th} and $(j + 1)^{\text{th}}$ node is as:

$$\begin{aligned}
& \left(\frac{1}{2a_{i,j}} \right) \bar{T}_{i-1,j}^y - \left(\frac{1}{2a_{i,j}} + \frac{1}{2a_{i+1,j}} \right) \bar{T}_{i,j}^y + \left(\frac{1}{2a_{i+1,j}} \right) \bar{T}_{i+1,j}^y \\
& = \left[a_{i,j} \left(\bar{S}_{1i,j}^{yx} - \bar{f}_{1i,j}^{yx} \right) + a_{i+1,j} \left(\bar{S}_{1i+1,j}^{yx} - \bar{f}_{1i+1,j}^{yx} \right) \right]
\end{aligned} \tag{3.4}$$

Similarly, the continuity equation at interface between j^{th} and $(j + 1)^{\text{th}}$ spatial nodes in y direction as shown in fig.3.4.

$$\bar{T}_{i,j}^x(+b_{i,j}) = \bar{T}_{i,j+1}^x(-b_{i+1,j})$$

The three-point scheme in y direction that relate j^{th} and $(j + 1)^{\text{th}}$ node is as:

$$\begin{aligned}
& \left(\frac{1}{2b_{i,j}} \right) \bar{T}_{i,j-1}^x - \left(\frac{1}{2b_{i,j}} + \frac{1}{2b_{i,j+1}} \right) \bar{T}_{i,j}^x + \left(\frac{1}{2b_{i,j+1}} \right) \bar{T}_{i,j+1}^x \\
& = \left[b_{i,j} \left(\bar{S}_{2i,j}^{xy} - \bar{f}_{1i,j}^{xy} \right) + b_{i,j+1} \left(\bar{S}_{2i,j+1}^{xy} - \bar{f}_{1i,j+1}^{xy} \right) \right]
\end{aligned} \tag{3.5}$$

The obscure pseudo-source terms are disposed off by implementing two constrained conditions. The first constraint equation is given by integrating eq. (3.1) by implementing operator that will result in relation between $\bar{S}_{1i,j}^{yx}$ and $\bar{S}_{2i,j}^{xy}$, which is as under:

$$\bar{S}_{1i,j}^{yx} + \bar{S}_{2i,j}^{xy} = \bar{f}_{1i,j}^{xy} \tag{3.6}$$

The last constraint equation is as:

$$\bar{T}_{i,j}^{x,y} = \bar{T}_{i,j}^{y,x} \tag{3.7}$$

If node dimension in x and y direction is constant, i.e.

$$\begin{aligned}
& +a_{i,j} = a_{i+1,j} = a \\
& +b_{i,j} = b_{i,j+1} = a
\end{aligned}$$

Solving equations (3.4), (3.5), (3.6), (3.7) and eliminating $\bar{S}_{1i,j}^{yx}$ and $\bar{S}_{2i,j}^{xy}$, we get the final set of two equations for two unknowns ($\bar{T}_{i,j}^x$ and $\bar{T}_{i,j}^y$) per node, which are as under:

$$\begin{aligned}
& \bar{T}_{i-1,j}^y \left(\frac{1}{2a^2} - \frac{1}{3(a^2 + b^2)} \right) - \bar{T}_{i,j}^y \left(\frac{1}{a^2} - \frac{1}{3(a^2 + b^2)} \right) + \bar{T}_{i+1,j}^y \left(\frac{1}{2a^2} - \frac{1}{2(a^2 + b^2)} \right) \\
& + \frac{3}{2} \left(\frac{\bar{T}_{i,j}^x + \bar{T}_{i,j-1}^x}{(a^2 + b^2)} \right) + \frac{3}{2} \left(\frac{\bar{T}_{i+1,j}^x + \bar{T}_{i+1,j-1}^x}{(a^2 + b^2)} \right) = - \left(\frac{b^2}{(a^2 + b^2)} \right) \{ \bar{f}_{1,i,j}^{xy} + \bar{f}_{1,i+1,j}^{xy} \}
\end{aligned} \tag{3.8}$$

$$\begin{aligned}
& \bar{T}_{i,j-1}^x \left(\frac{1}{2a^2} - \frac{1}{3(a^2 + b^2)} \right) - \bar{T}_{i,j}^x \left(\frac{1}{a^2} - \frac{1}{3(a^2 + b^2)} \right) + \bar{T}_{i,j+1}^x \left(\frac{1}{2a^2} - \frac{1}{2(a^2 + b^2)} \right) \\
& + \frac{3}{2} \left(\frac{\bar{T}_{i,j}^y + \bar{T}_{i-1,j}^y}{(a^2 + b^2)} \right) + \frac{3}{2} \left(\frac{\bar{T}_{i,j+1}^y + \bar{T}_{i-1,j+1}^y}{(a^2 + b^2)} \right) = - \left(\frac{a^2}{(a^2 + b^2)} \right) \{ \bar{f}_{1,i,j}^{xy} + \bar{f}_{1,i,j+1}^{xy} \}
\end{aligned} \tag{3.9}$$

where $\bar{T}_{i,j}^x$ and $\bar{T}_{i,j}^y$ are space averaged temperatures in x and y direction as shown in fig.3.2.

a and b are mesh spacing in x and y directions respectively.

3.2 Discretized Steady State 2-D Diffusion Equation with Heat Source:

By following pre-defined steps, we obtain following set of discretized equations: -

$$\begin{aligned}
& \bar{T}_{i,j}^x \\
& = \frac{(\bar{T}_{i+1,j}^x + \bar{T}_{i-1,j}^x) \left(\frac{1}{2b^2} - \frac{3}{2(a^2 + b^2)} \right) + \left(\frac{3}{2(a^2 + b^2)} \right) (\bar{T}_{i,j}^y + \bar{T}_{i-1,j}^y + \bar{T}_{i,j+1}^y + \bar{T}_{i-1,j+1}^y) + \left(\frac{4a^2}{a^2 + b^2} \right)}{\left(\frac{1}{b^2} + \frac{3}{(a^2 + b^2)} \right)}
\end{aligned} \tag{3.10}$$

$$\begin{aligned}
& \bar{T}_{i,j}^y \\
& = \frac{(\bar{T}_{i,j+1}^y + \bar{T}_{i,j-1}^y) \left(\frac{1}{2b^2} - \frac{3}{2(a^2 + b^2)} \right) + \left(\frac{3}{2(a^2 + b^2)} \right) (\bar{T}_{i,j}^x + \bar{T}_{i,j-1}^x + \bar{T}_{i+1,j}^x + \bar{T}_{i+1,j-1}^x) + \left(\frac{4b^2}{a^2 + b^2} \right)}{\left(\frac{1}{a^2} + \frac{3}{(a^2 + b^2)} \right)}
\end{aligned} \tag{3.11}$$

where $\bar{T}_{i,j}^x$ and $\bar{T}_{i,j}^y$ are space averaged temperatures in x and y direction. a and b are mesh spacing in

x and y directions respectively.

3.3 Discretized 1D Convection Diffusion Equation:

Following as in previous section, given set of discretized equations is obtained:

$$\bar{T}_{i,j}^x = \frac{\left(\frac{X + dt}{dt}\right) (\bar{T}_{i,j-1}^x) - \left((2 * B) * (\bar{T}_{i,j}^t)\right) - \left((2 * A) * (\bar{T}_{i+1,j}^t)\right)}{\left(\frac{X - dt}{dt}\right)} \quad (3.12)$$

$$\bar{T}_{i,j}^t = \frac{\left(\frac{G * (\bar{T}_{i-1,j}^x + \bar{T}_{i-1,j-1}^x)}{(2 * X) * \alpha}\right) + \left(\frac{(2 * dx * A)(\bar{T}_{i,j}^x + \bar{T}_{i,j-1}^x)}{(2 * X) * \alpha}\right) - \left((D * \bar{T}_{i-1,j}^t) - F * \bar{T}_{i+1,j}^t\right)}{E} \quad (3.13)$$

where X, A, B, G, D, E, F, α are pre-defined constants. $\bar{T}_{i,j}^x$ and $\bar{T}_{i,j}^t$ are space average and time averaged temperatures respectively.

3.4 Discretized Steady State 2-D Convection-Diffusion Equation with Heat Source:

$$\bar{T}_{i,j}^y = \frac{\bar{T}_{i-1,j}^y \left(\frac{1}{2a^2} - \frac{1}{3(a^2 + b^2)}\right) + \bar{T}_{i+1,j}^y \left(\frac{1}{2a^2} - \frac{1}{2(a^2 + b^2)}\right)}{\left(\frac{1}{a^2} - \frac{1}{3(a^2 + b^2)}\right)} + \frac{\frac{3}{2} \left(\frac{\bar{T}_{i,j}^x + \bar{T}_{i,j-1}^x}{(a^2 + b^2)}\right) + \frac{3}{2} \left(\frac{\bar{T}_{i+1,j}^x + \bar{T}_{i+1,j-1}^x}{(a^2 + b^2)}\right) + \left(\frac{b^2}{(a^2 + b^2)}\right) \{\bar{f}_{1,i,j}^{xy} + \bar{f}_{1,i+1,j}^{xy}\}}{\left(\frac{1}{a^2} - \frac{1}{3(a^2 + b^2)}\right)} \quad (3.14)$$

$$\begin{aligned} \bar{T}_{i,j}^x = & \frac{\bar{T}_{i,j-1}^x \left(\frac{1}{2a^2} - \frac{1}{3(a^2 + b^2)} \right) + \frac{3}{2} \left(\frac{\bar{T}_{i,j}^y + \bar{T}_{i-1,j}^y}{(a^2 + b^2)} \right) + \frac{3}{2} \left(\frac{\bar{T}_{i,j+1}^y + \bar{T}_{i-1,j+1}^y}{(a^2 + b^2)} \right)}{\left(\frac{1}{a^2} - \frac{1}{3(a^2 + b^2)} \right)} \\ & + \frac{\bar{T}_{i,j+1}^x \left(\frac{1}{2a^2} - \frac{1}{2(a^2 + b^2)} \right) + \left(\frac{a^2}{(a^2 + b^2)} \right) \{ \bar{f}_{1,i,j}^{xy} + \bar{f}_{1,i,j+1}^{xy} \}}{\left(\frac{1}{a^2} - \frac{1}{3(a^2 + b^2)} \right)} \end{aligned} \quad (3.15)$$

where $\bar{T}_{i,j}^x$ and $\bar{T}_{i,j}^y$ are space averaged temperatures in x and y direction respectively.
a and b are mesh spacing in x and y directions respectively.

3.5 Discretized Non-linear Equations (Navier-Stokes)

Again, scheme for Navier-Stokes conditions is created with reference to the plan produced for the convection diffusion condition as talked about in previous section. The crude type of two-dimensional relentless state Navier-Stokes conditions in global coordinate system is:

$$\frac{\partial \hat{u}}{\partial x} + \frac{\partial \hat{v}}{\partial y} = 0 \quad (3.17)$$

$$\mathbf{u} \frac{\partial \hat{u}}{\partial x} + \mathbf{v} \frac{\partial \hat{u}}{\partial y} - \mathbf{v} \left\{ \frac{\partial^2 \hat{u}}{\partial x^2} + \frac{\partial^2 \hat{u}}{\partial y^2} \right\} - \frac{1}{p} \frac{\partial \hat{p}}{\partial x} + \hat{\mathbf{b}}_x = 0 \quad (3.18)$$

$$\mathbf{u} \frac{\partial \hat{v}}{\partial x} + \mathbf{v} \frac{\partial \hat{v}}{\partial y} - \mathbf{v} \left\{ \frac{\partial^2 \hat{v}}{\partial x^2} + \frac{\partial^2 \hat{v}}{\partial y^2} \right\} - \frac{1}{p} \frac{\partial \hat{p}}{\partial y} + \hat{\mathbf{b}}_y = 0 \quad (3.19)$$

where x; y are the independent spatial variables and \hat{b}_x ; \hat{b}_y are the body force term in x and y direction respectively. The \hat{u} , \hat{v} and p are velocity components and pressure in global domain. The continuity condition is oftenly replaced by the elliptic form of pressure Poisson equation.

The pressure Poisson equation in terms of pressure correction p' is:

$$\frac{\partial^2 p'}{\partial x^2} + \frac{\partial^2 p'}{\partial y^2} = \frac{\partial u^*}{\partial x} + \frac{\partial v^*}{\partial y} \quad (3.20)$$

Eqs. (3.18 and 3.19) along with Eq. (3.20) are mathematically similar to the set of Eqs. (3.17, 3.18

and 3.19). Since N-S equations are non-linear in nature the convective terms of the equations are approximated to produce cell analytical solution. These approximations are incorporated by taking the cell averaged velocity in convection terms of the N-S equations which are defined as:

$$\bar{u}_c(i,j) = \frac{\bar{u}_{i,j}^\eta + \bar{u}_{i+1,j}^\eta + \bar{u}_{i,j}^\xi + \bar{u}_{i,j+1}^\xi}{4} \quad (3.21)$$

$$\bar{v}_c(i,j) = \frac{\bar{v}_{i,j}^\eta + \bar{v}_{i+1,j}^\eta + \bar{v}_{i,j}^\xi + \bar{v}_{i,j+1}^\xi}{4} \quad (3.22)$$

With reference to the Figure 2.5, the cell average velocities for (i, j) th cell are calculated by taking the mean of cell surface velocities (Eq. (5.5)). These approximations are verified and tested in the previously schemes for N-S equations by Kai et al. [24] and Kumar et al. [13]. This leads, linear form of governing N-S equations similar to the convection diffusion equation.

$$\nabla \nabla V \approx V_c \nabla \nabla V$$

After linearization of convection terms, the N-S equations can be written as:

$$u_c \frac{\partial u}{\partial x} + v_c \frac{\partial u}{\partial y} - \nu \left[\frac{\partial^2 u}{\partial x^2} + \frac{\partial^2 u}{\partial y^2} \right] + \frac{1}{\rho} \frac{\partial p}{\partial x} + g_x(x, y) = 0 \quad (3.23)$$

$$u_c \frac{\partial v}{\partial x} + v_c \frac{\partial v}{\partial y} - \nu \left[\frac{\partial^2 v}{\partial x^2} + \frac{\partial^2 v}{\partial y^2} \right] + \frac{1}{\rho} \frac{\partial p}{\partial y} + g_y(x, y) = 0 \quad (3.24)$$

where the velocity u_c is cell-averaged u velocity or representative u velocity for a particular cell.

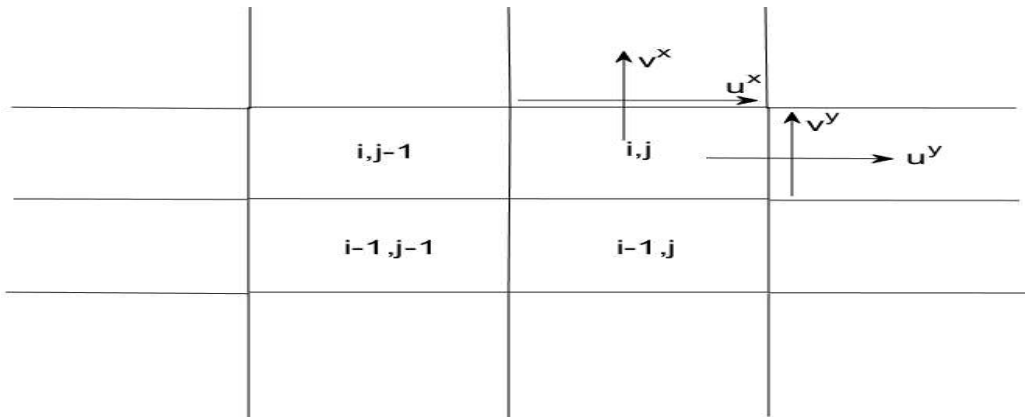


Figure 3. 5 : Transverse averaged velocity components on x and y surfaces respectively.

Now equations (3.23 and 3.24) [12] are discretized over a spatial domain in the same manner as given in mathematical formulation to get transverse averaged quantities on x and y face of a nodal cell as shown in fig. 3.5, defined as below:

$$\bar{p}_{ij}^x = \frac{F_{11}\bar{p}_{i,j-1}^x + F_{13}\bar{p}_{i,j+1}^x + F_{14}(\bar{p}_{ij}^y + \bar{p}_{i-1,j}^y) + F_{15}(\bar{p}_{i,j+1}^y + \bar{p}_{i-1,j+1}^y) - F_{16}f_{1ij} - F_{17}f_{1i,j+1}}{F_{12}} \quad (3.25)$$

$$\bar{p}_{ij}^y = \frac{F_{21}\bar{p}_{i-1,j}^y + F_{23}\bar{p}_{i+1,j}^y + F_{24}(\bar{p}_{ij}^x + \bar{p}_{ij-1}^x) + F_{25}(\bar{p}_{i+1,j}^x + \bar{p}_{i+1,j-1}^x) - F_{26}f_{1ij} - F_{27}f_{1i+1,j}}{F_{22}} \quad (3.26)$$

$$\bar{u}_{ij}^x = \frac{F_{31}\bar{u}_{i,j-1}^x + F_{33}\bar{u}_{i,j+1}^x + F_{34}\bar{u}_{i-1,j}^y + F_{35}\bar{u}_{ij}^y - F_{36}\bar{u}_{i-1,j+1}^y - F_{37}\bar{u}_{i,j+1}^y - F_{38}f_{2ij} + F_{39}f_{2i,j+1}}{F_{32}} \quad (3.27)$$

$$\bar{u}_{ij}^y = \frac{F_{41}\bar{u}_{i-1,j}^y + F_{43}\bar{u}_{i+1,j}^y + F_{44}\bar{u}_{ij-1}^x + F_{45}\bar{u}_{ij}^x - F_{46}\bar{u}_{i+1,j-1}^x - F_{47}\bar{u}_{i+1,j}^x - F_{48}f_{2ij} + F_{49}f_{2i+1,j}}{F_{42}} \quad (3.28)$$

$$\bar{v}_{ij}^x = \frac{F_{31}\bar{v}_{i,j-1}^x + F_{33}\bar{v}_{i,j+1}^x + F_{34}\bar{v}_{i-1,j}^y + F_{35}\bar{v}_{ij}^y - F_{36}\bar{v}_{i-1,j+1}^y - F_{37}\bar{v}_{i,j+1}^y - F_{38}f_{2ij} + F_{39}f_{2i,j+1}}{F_{32}} \quad (3.29)$$

$$\bar{v}_{ij}^y = \frac{F_{41}\bar{v}_{i-1,j}^y + F_{43}\bar{v}_{i+1,j}^y + F_{44}\bar{v}_{ij-1}^x + F_{45}\bar{v}_{ij}^x - F_{46}\bar{v}_{i+1,j-1}^x - F_{47}\bar{v}_{i+1,j}^x - F_{48}f_{2ij} + F_{49}f_{2i+1,j}}{F_{42}} \quad (3.30)$$

CHAPTER 4

NUMERICAL RESULTS AND DISCUSSIONS

4.1 STEADY STATE 2D DIFFUSION

Problem Description

Find the solution of poisson's equation, $\nabla^2 T = -2$, in square with boundary conditions,

1. $T(0, y) = 0$;
2. $T(L, y) = 0$;
3. $T(x, 0) = 0$;
4. $T(x, L) = 0$;

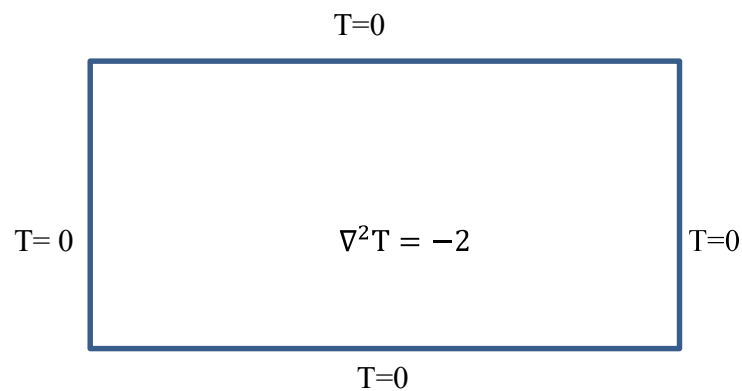


Figure 4. 1 : Implemented boundary conditions for given problem domain

Table 4. 1 : Comparison between relative error for solutions obtained utilizing FDM and NIM with respect to analytical solution

NO. OF NODES	COMPARISON WITH ANALYTICAL SOLUTION (RELATIVE ERROR)	
	FDM	NIM
4×4	0.25	0.0180
8×8	0.125	0.0034
12×12	0.0833	0.0017

In the above table, for given steady state 2d diffusion problem, it can be viewed that as the grid size increases, the error is decreasing for both FDM and NIM. It is easily noticeable that for any grid size, the NIM give efficient results with error less than tenth order times less as compared to error generated utilizing FDM. So, for coarser meshes like 4x4 and 8x8, NIM proves to be far better in converging to very low error values as compared to FDM.

4.2 1D CONVECTION DIFFUSION

ProblemDescription

For the convection diffusion in one dimensional domain initial temperature distribution in the flow domain is $T(x,0)=e^{-\frac{(x-x_0)^2}{\sigma}}$, and the boundary conditions are $x(0,t)=0$ and $x(L,t)=0$. The data are $L=5m$, $u=2m/s$, $\alpha=0.1m^2/s$, $\sigma=0.01m$. Find the solution and compare with analytical result.

Table 4. 2 : Comparison between relative error for solutions obtained utilizing FDM and NIM with respect to analytical solution

NO. OF NODES	COMPARISON WITH ANALYTICAL SOLUTION (RELATIVE ERROR)	
	FDM	NIM
40	0.3422	0.0187
50	0.1456	0.0191
60	0.0965	0.0125

In the table-2, for given 1d convection diffusion issue, it tends to be seen that as the grid size expands,

the error is diminishing for both FDM and NIM. It is effectively detectable that for any matrix measure, the NIM give productive outcomes with error under tenth order when contrasted with error generate using FDM. Thus, again in this case, for coarser lattices like 40x40, NIM demonstrates to be far superior in uniting to extremely low error values when contrasted with FDM. It is also noticeable that as grid size is increasing, the difference between errors given by NIM and FDM respectively, is decreasing.

4.3 STEADY STATE 2D CONVECTION-DIFFUSION

Problem Description (Case-1)

Analytic solution, zero source term, constant vertical wind, exponential boundary layer. The function

$$u(x, y) = \frac{1 - e^{1-y/\alpha}}{1 - e^{-2/\alpha}}$$

given that $\vec{\omega} = (0, 1)$ (velocity vector)

dirichlet conditions on the boundary are determined as given below:

$$u(x, -1) = x, u(x, 1) = 0$$

$$u(-1, y) = -1, u(1, y) = 1$$

Table 4. 3 : Comparison between relative error for solutions obtained utilizing FDM and NIM with respect to analytical solution

NO. OF NODES	COMPARISON WITH ANALYTICAL SOLUTION (RELATIVE ERROR)	
	FDM	NIM
4x4	0.25	0.125
8x8	0.125	0.093
16x16	0.062	0.05
32x32	0.03	0.025

In table-3, for the given case-1 of steady state 2d convection-diffusion, again we can see that the error given by NIM scheme is far less as compared to that given by FDM. As in previous defined cases, NIM generate low converging error values for coarser mesh sizes like 4x4 and 8x8, i.e. approximately two times less than the results produced utilizing FDM.

Problem Description (Case-2)

To obtain temperature distribution T in region ABCD (2x2) between two plates with a constant heat flux q imposed on both plates. The flow velocity is given by:

$$u(y) = \frac{3}{2} \times \bar{u} \left[1 - \left(\frac{y}{h} \right)^2 \right]$$

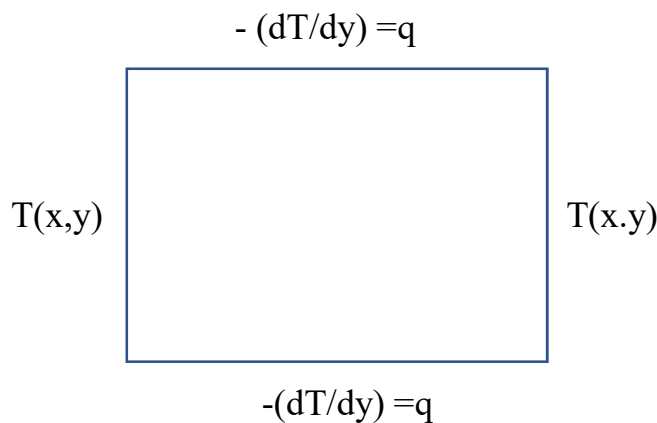


Figure 4. 2 : Implemented boundary conditions for given problem domain

boundary conditions: -(shown in fig. 4.2)

1. $-(dT/dx) = q$, on both upper and lower boundary
2. on side faces,

$$T(x, y) = \left(\frac{q \times h}{k} \right) \left[\left(\frac{3}{4} \right) \left(\frac{y}{h} \right)^2 \left(1 - \frac{y^2}{6 \times h^2} \right) + \left(\frac{4}{Pev} \right) \left(\frac{x}{h} \right) \right]$$

where $h=1$, $Pev=Re \times Pr$, $Re=1$, $Pr=0.7$

Table 4. 4 : Comparison between relative error for solutions obtained utilizing FDM and NIM with respect to analytical solution

NO. OF NODES	COMPARISON WITH ANALYTICAL SOLUTION (RELATIVE ERROR)	
	FDM	NIM
24x24	2.54×10^{-4}	1.988×10^{-6}
36x36	1.091×10^{-4}	4.588×10^{-7}
48x48	1.091×10^{-4}	1.599×10^{-7}

In the table-4, for given case-2 of steady state 2d convection-diffusion, the error produced by NIM is very far less as contrasted with that of FDM. i.e. approximately tenth raised to power two, times less. The NIM again generate very low converging error for coarse grid size like 24x24, as compared with FDM. In the given case, the NIM produced error with comparison to FDM, is very low as compared to previous cases. Thus, NIM scheme proves to be more efficient and less tedious than FDM in all given cases.

4.4 LID DRIVEN CAVITY WITH SQUARE SHAPED OBSTACLE AT CENTER

The given problem has been modeled using discretized N-S equations utilizing NIM successfully. The lid driven cavity problem has been taken into account to see the change in velocity distribution and flow physics, introduced due to the different sizes of square shaped blockage placed at center, at different grid sizes (40x40 and 50x50) and reynold number (100,400 and 1000) leading to six different cases. The applied boundary conditions at the lid and blockage surface are shown in figure given below: -

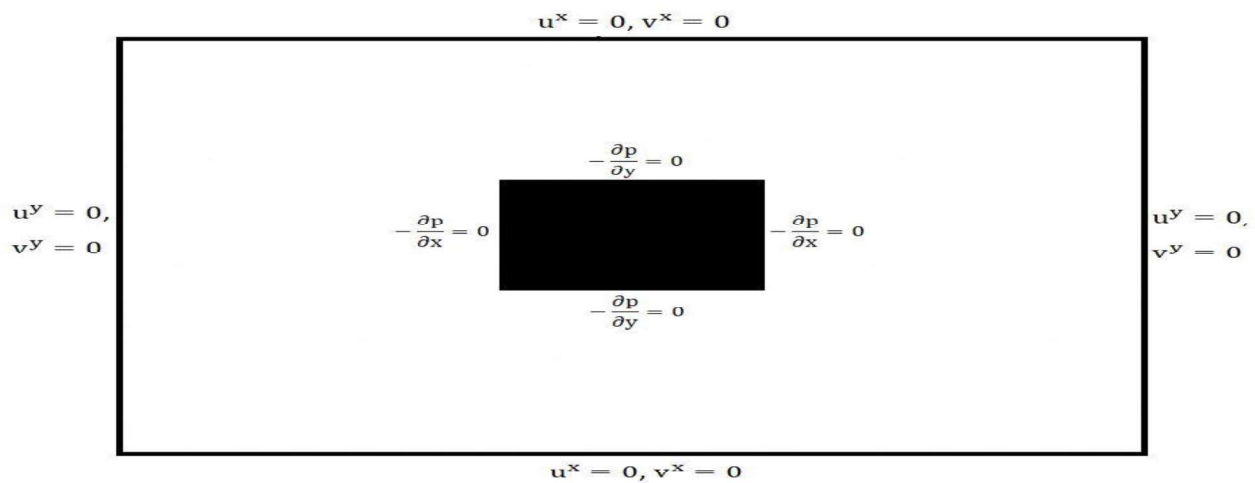


Figure 4. 3 : Implemented boundary conditions at lid and blockage surface

We have considered two problems of square shaped lid driven cavity with square shaped obstacle of length (0.1, 0.2) of total length of lid driven cavity. The following effects have been observed on flow physics as shown in figs. given below:

Case-1: With blockage size (0.1 of the total length of lid driven cavity) and reynold number (Re=1000)

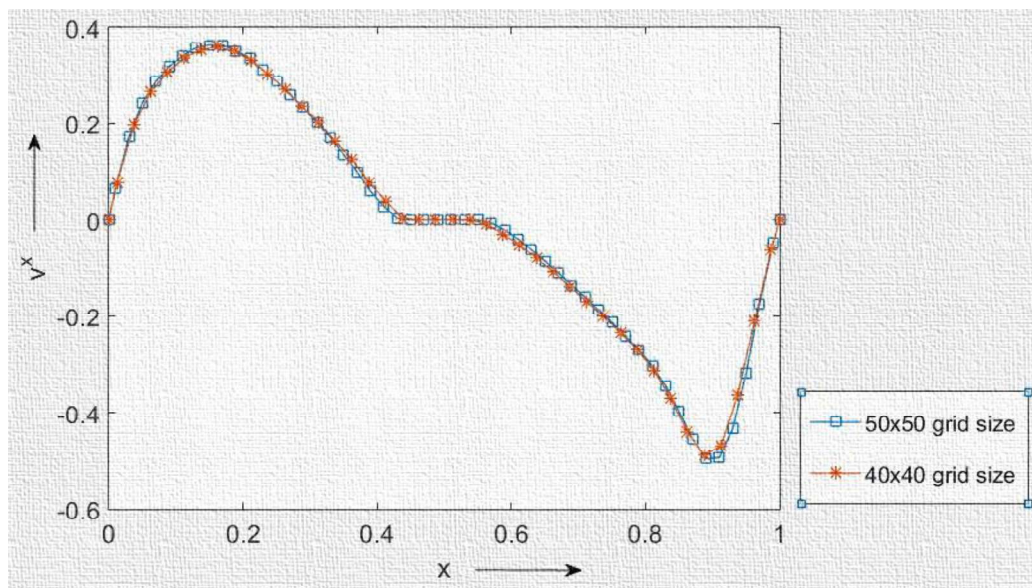


Figure 4. 4 : Plot showing comparison in variation of transverse averaged velocity component (v^x) distribution in x-direction at blockage size (0.1 of the total length of cavity) and Re=1000

The above figure shows that the transverse averaged velocity component v^x at the horizontal geometric centerline of cavity, which follows exactly the same trend or shows negligible change for same reynold number 1000 and same blockage size at different grid sizes(50x50 and 40x40).From the above figure, we can infer that the defined velocity component v^x , for different defined grid sizes and given constant reynold number and blockage size, first increases till $x=0.4$, due to positive velocity gradient and from $x=0.4$ onwards, till $x=0.6$,it becomes constantly zero due to no slip condition at obstacle wall and no velocity inside solid obstacle. Now when the obstacle wall ends from $x=0.6$ onwards to $x=0.9$, the velocity shows negative trend as we are moving in the direction opposite to flow (negative velocity gradient). Finally, at the cavity wall at $x=1$, the velocity becomes zero again due to implemented boundary condition there.

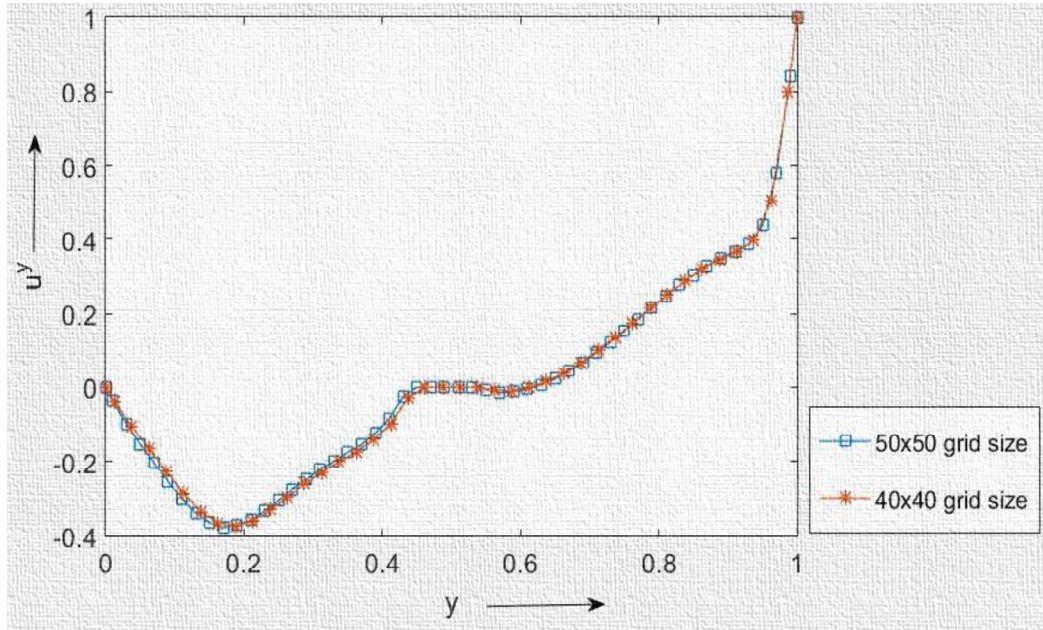


Figure 4. 5 : Plot showing comparison in variation of transverse averaged velocity component (u^y) distribution in y -direction at blockage size (0.1 of the total length of cavity) and $Re=1000$

From the above figure, we conclude that the transverse averaged velocity component u^y at the geometric vertical centerline of cavity follows exactly the same pattern for different defined grid sizes at same given blockage size and reynold number.i.e. it first decreases till $x=0.2$ due to negative velocity gradient.

After that it increases till $x=0.45$ and reaches zero due to no slip condition at the the obstacle wall and till $x=0.6$, remains constantly zero until obstacle wall ends. Now after $x=0.6$, the velocity u^y shows increasing trend due to positive velocity gradient.

Case-2: With blockage size (0.1 of total length of lid driven cavity) and reynold number (Re=400)

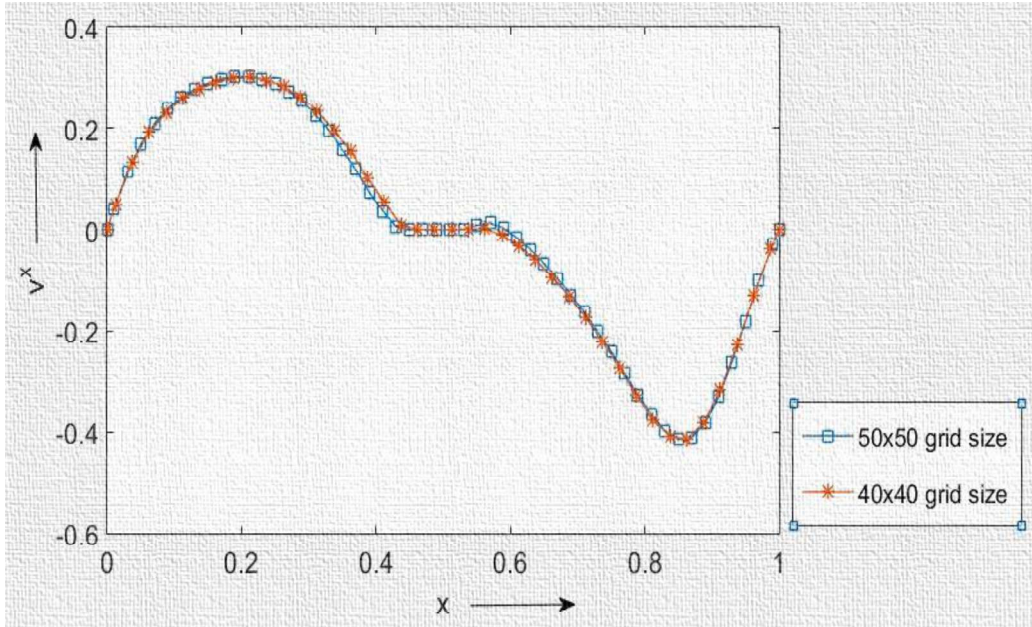


Figure 4. 6 : Plot showing comparison in variation of transverse averaged velocity component (v^x) distribution in x-direction at blockage size (0.1 of the total length of cavity) and Re=400

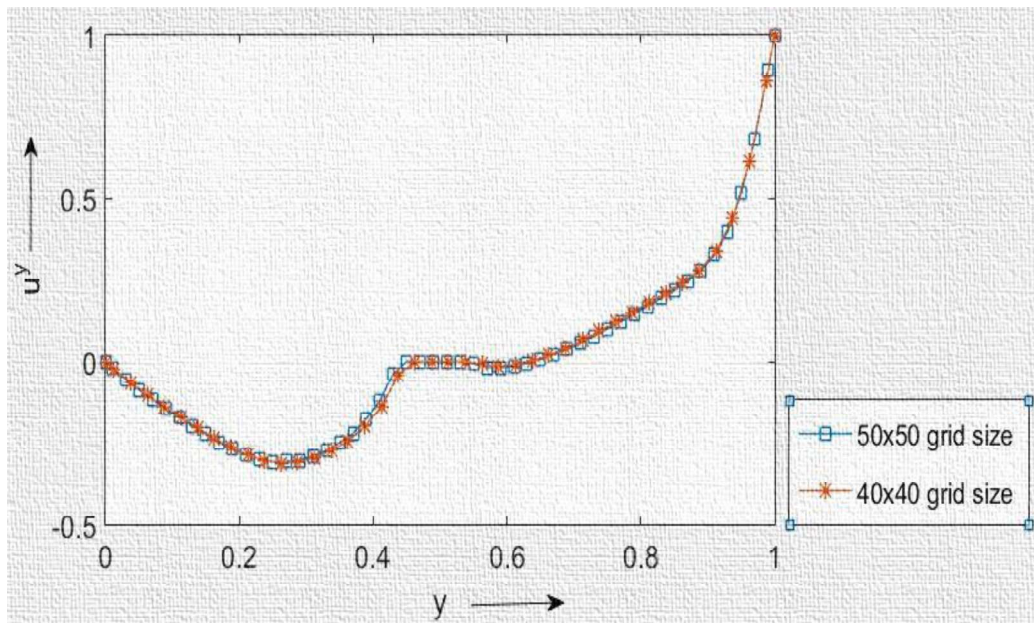


Figure 4. 7 : Plot showing comparison in variation of transverse averaged velocity component (u^y) distribution in y-direction at blockage size (0.1 of the total length of cavity) and Re=400

For the above given case, the velocity profiles for both components v^x and u^y at the geometric horizontal and vertical centerline of cavity respectively, follows the same trend respectively as discussed in previous case. But due to decrease in reynold number from 1000 to 400 for same given blockage size, the increase noticed in velocity component v^x till $x=0.2$, is less.i.e. in previous case, it is nearly touching 0.4 and in the given case, it reaches till 0.3. From $x=0.2$, it decreases as it approaches blockage wall, due to no slip condition. After that it decreases from zero to negative due to negative velocity gradient but in this case, the downfall is till 0.4 which is 0.5 for previous case, again due to low defined reynold number compared to previous case. Now same is the case with velocity component, u^y for which up fall noticed in this case is not so sharp or linear as the curve in previous case. Also, downfall noticed is less as for v^x , due to lower given reynold number in latter cases.

Case-3: With blockage size (0.1 of total length of lid driven cavity and reynold number (Re=100))

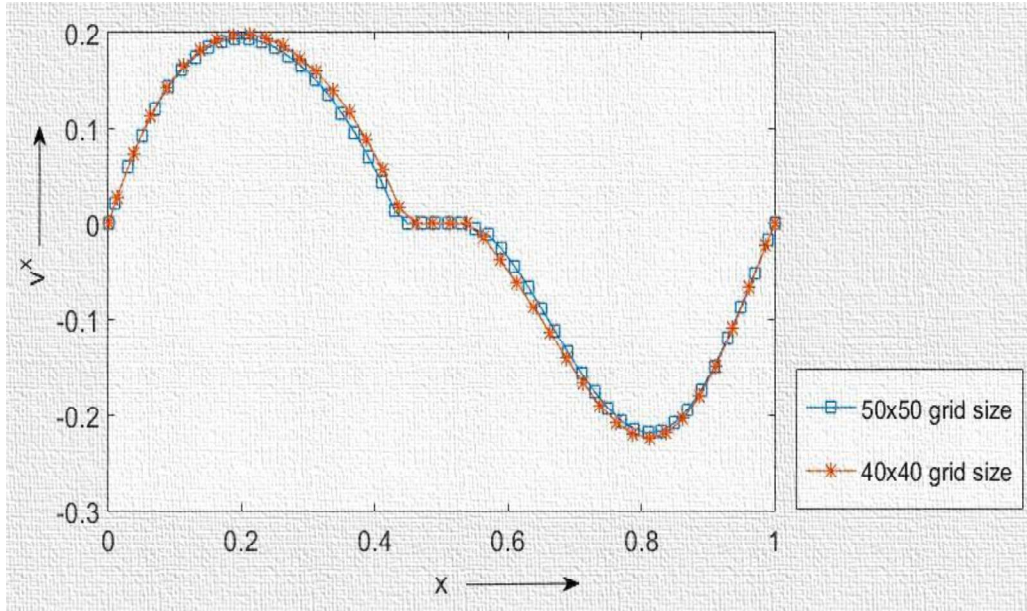


Figure 4. 8 : Plot showing comparison in variation of transverse averaged velocity component (v^x) distribution in x-direction at blockage size (0.1 of the total length of cavity) and Re=100

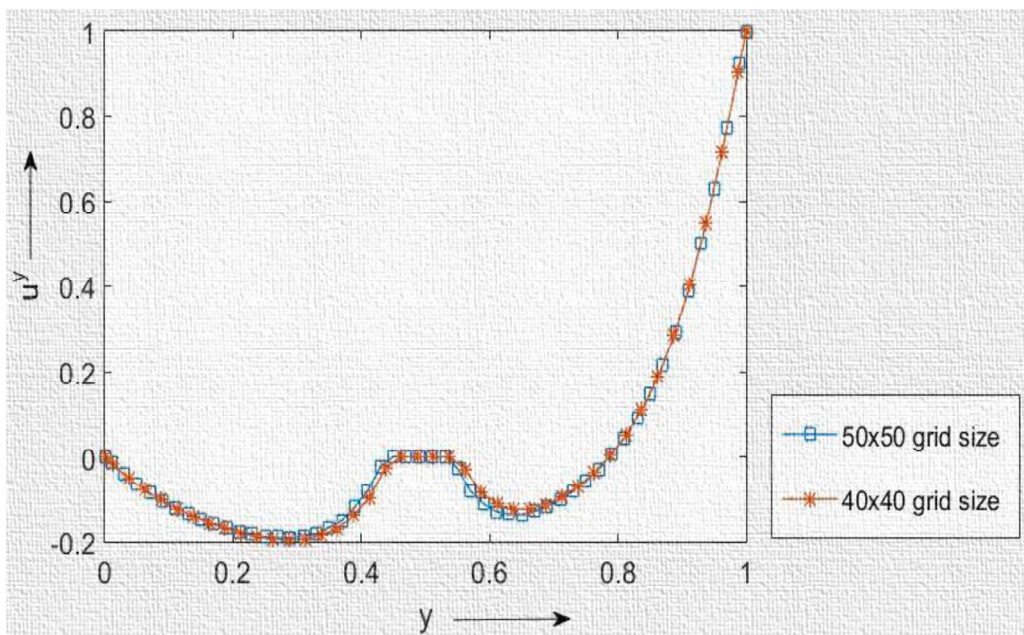


Figure 4. 9 : Plot showing comparison in variation of transverse averaged velocity component (u^y) distribution in y-direction at blockage size (0.1 of the total length of cavity) and Re=100

Case-4: With blockage size (0.2 of total length of lid driven cavity) and reynold number (Re=1000)

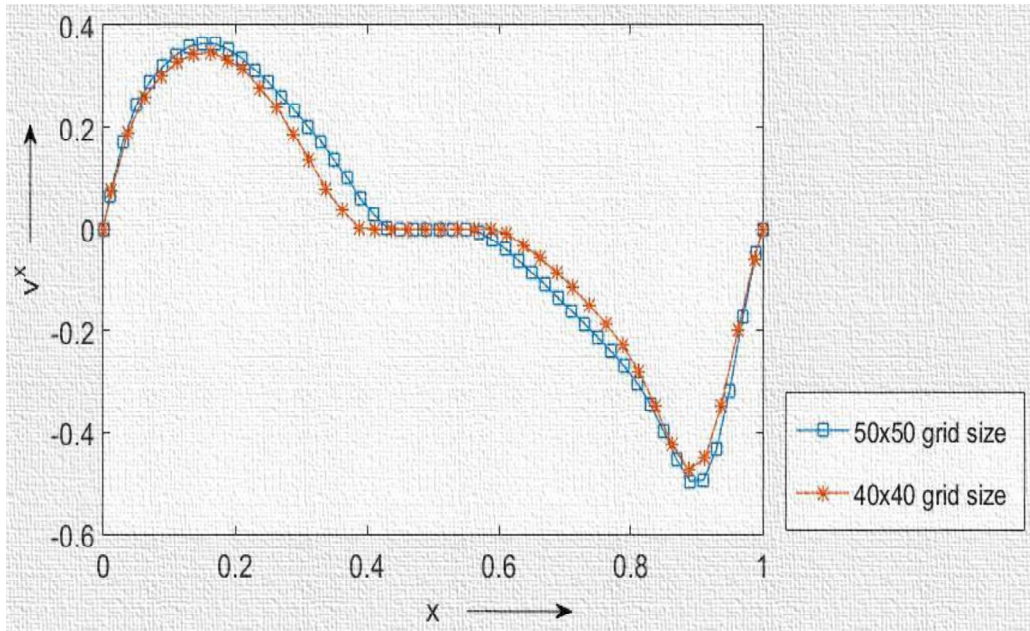


Figure 4. 10 : Plot showing comparison in variation of transverse averaged velocity component (v^x) distribution in x-direction at blockage size (0.2 of the total length of cavity) and Re=1000

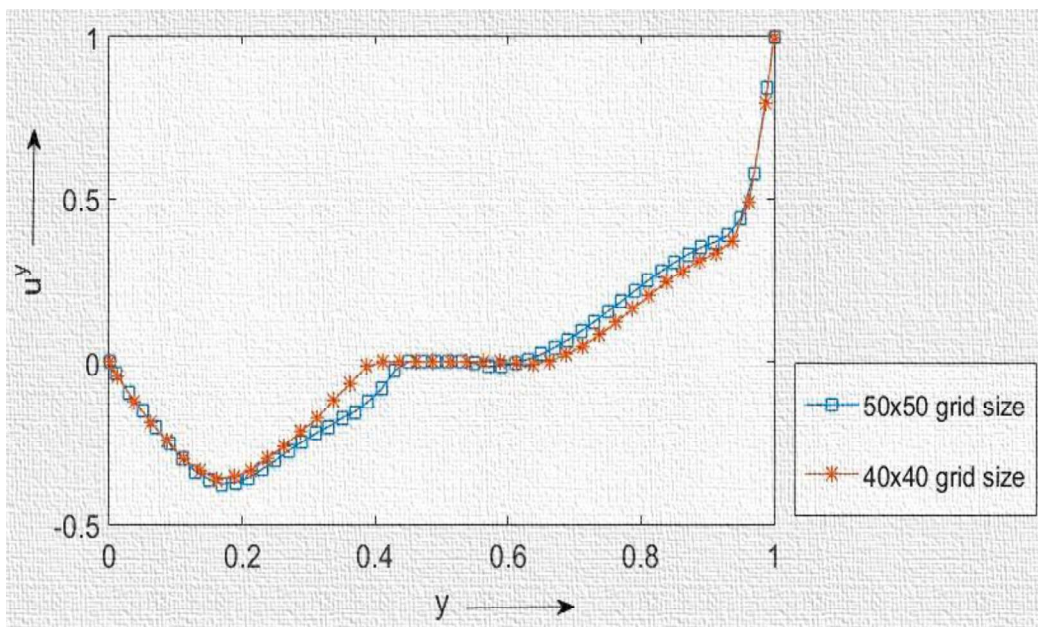


Figure 4. 11 : Plot showing comparison in variation of transverse averaged velocity component (u^y) distribution in y-direction at blockage size (0.2 of the total length of cavity) and Re=1000

Case-5: With blockage size (0.2 of total length of lid driven cavity) and reynold number (Re=400)

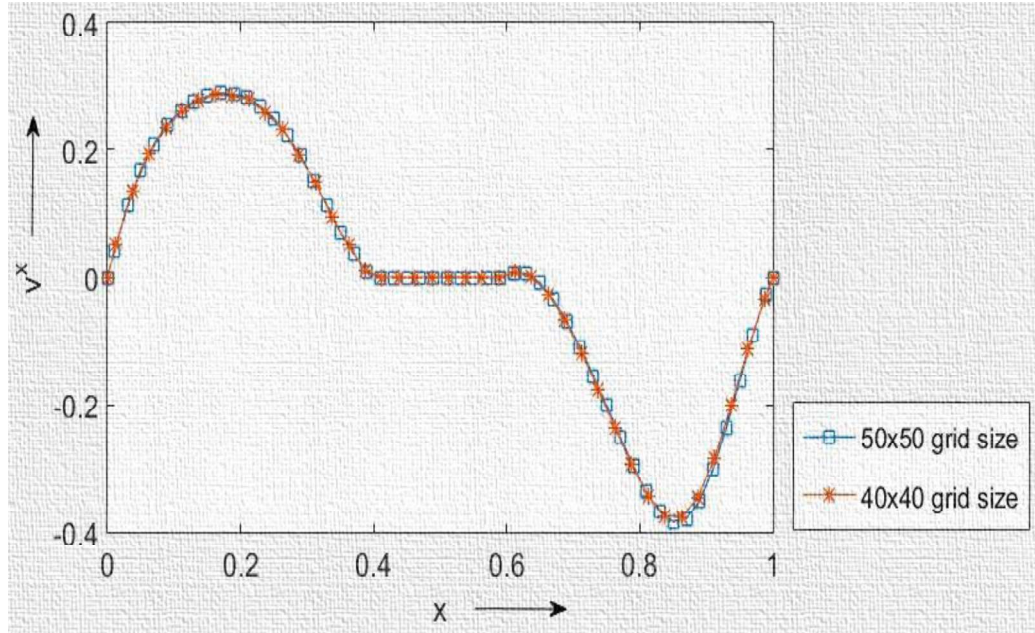


Figure 4. 12 : Plot showing comparison in variation of transverse averaged velocity component (v^x) distribution in x-direction at blockage size (0.2 of the total length of cavity) and Re=400

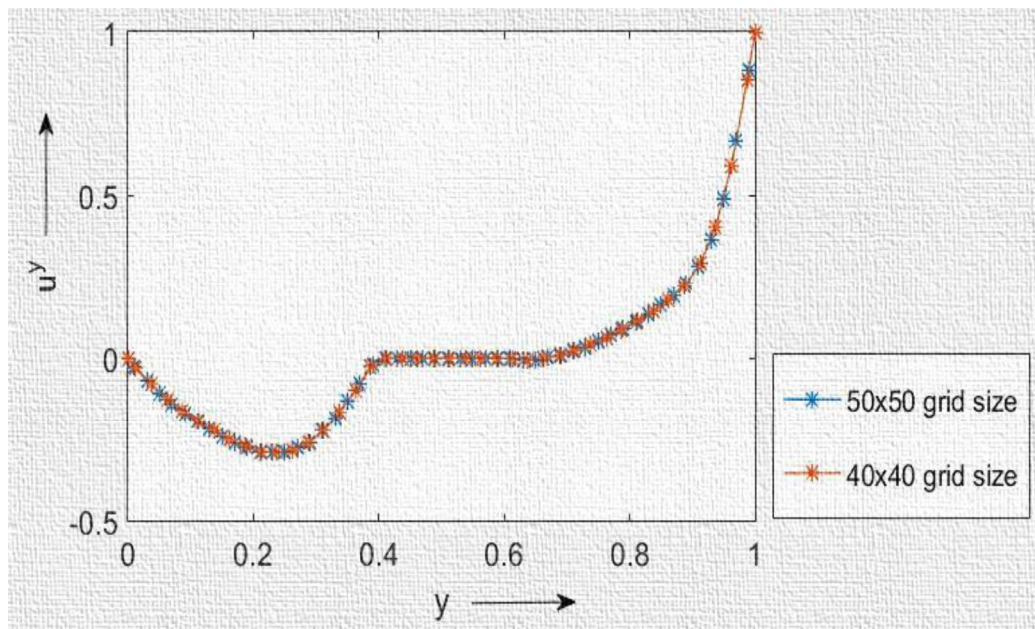


Figure 4. 13 : Plot showing comparison in variation of transverse averaged velocity component (u^y) distribution in y-direction at blockage size (0.2 of the total length of cavity) and Re=400

Case-6: With blockage size (0.2 of total length of lid driven cavity) and reynold number (Re=100)

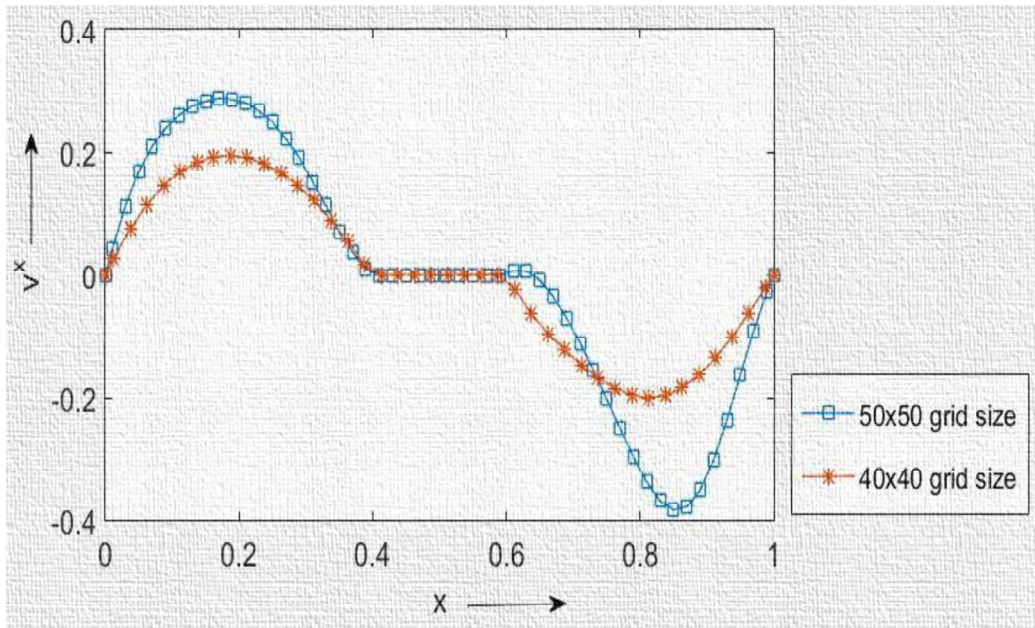


Figure 4. 14 : Plot showing comparison in variation of transverse averaged velocity component (v^x) distribution in x-direction at blockage size (0.2 of the total length of cavity) and Re=100

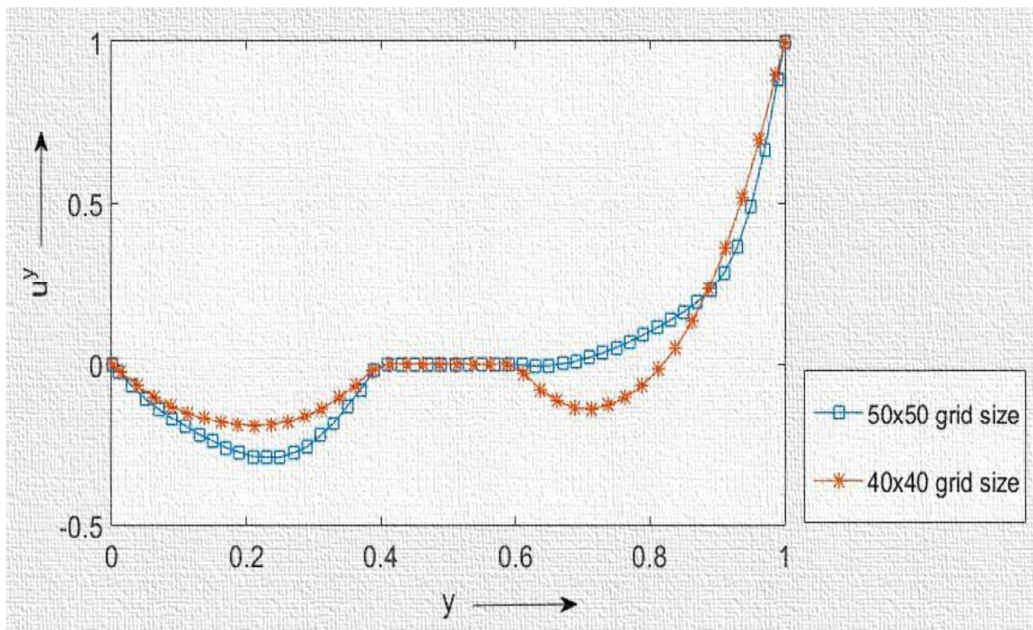


Figure 4. 15 : Plot showing comparison in variation of transverse averaged velocity component (u^y) distribution in y-direction at blockage size (0.2 of the total length of cavity) and Re=100

Now for all the defined cases from case 4 to case 6, the velocity profiles for v^x and u^y are almost following the same trend as depicted in previous three cases but due to increased blockage size (from

0.1 to 0.2 of the total length of cavity), the deviation between curves is not negligible as in previous cases except case 5, where they are exactly similar. The up fall for v^x decreases from 0.4 to 0.3, due to low defined reynold number in case 5 as compared to case 4. The downfall also decreases from -0.5 to -0.4, as the given cases 4 and 5, are compared. The downfall and up fall in v^x do not decrease for case 6 as the reynold number is decreased to 100, and it looks like that it is not more dependent on reynold number unless the blockage size variates. The velocity component u^y also show the similar downward trend as the downfall decreases from -0.4 to -0.3 and remains same or constant at -0.3 for the last case, and decrease in reynold number from 400 to 100, has a very little implication on value of component u^y as for v^x , showing that reynold number being less significant and blockage size is playing a crucial role in any deviation observed at lower reynold numbers. The upward trend is more sharp or linear for u^y in case 4 and becomes less linear as for case 5 and 6, as reynold number keeps decreasing.

Stream Function Plots for grid size(50x50)

The stream function is defined for incompressible flows in two dimensions. The difference between the stream function values at any two points gives the volumetric flow rate (or volumetric flow rate) through a line connecting the two points.

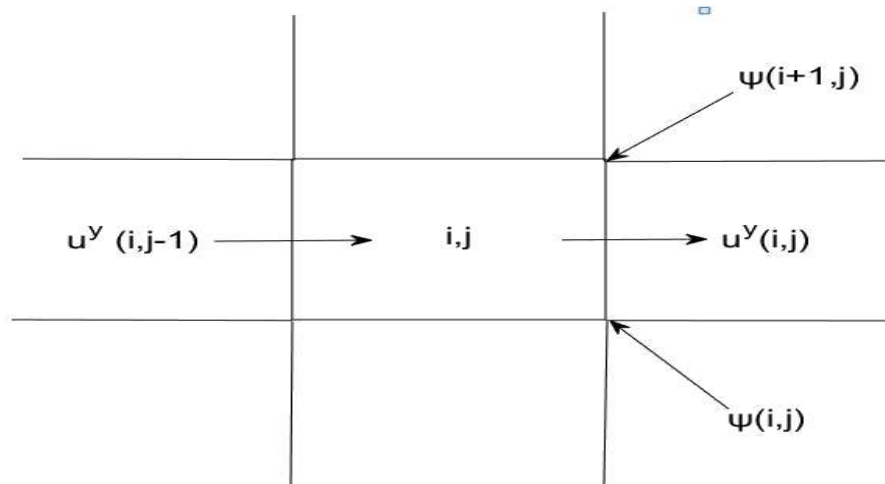


Figure 4. 16 : Stream function defined at respective nodes in problem domain

Generally, the stream function is defined as below: -

$$\frac{\partial \psi}{\partial y} = u$$

In our terminology here, we can write it as: -

$$\psi(i + 1, j) = \{ [u^y(i, j)] \times dy \} + \psi(i, j)$$

We have plotted contours for six different cases at 50x50 grid size at Reynold number (Re=1000,400,100) and corresponding obstacle sizes, to show the trajectories of flow through problem domain at discrete nodal points.

Case-1: With blockage size (0.1 of the total length of lid driven cavity) and reynold number (Re=1000)

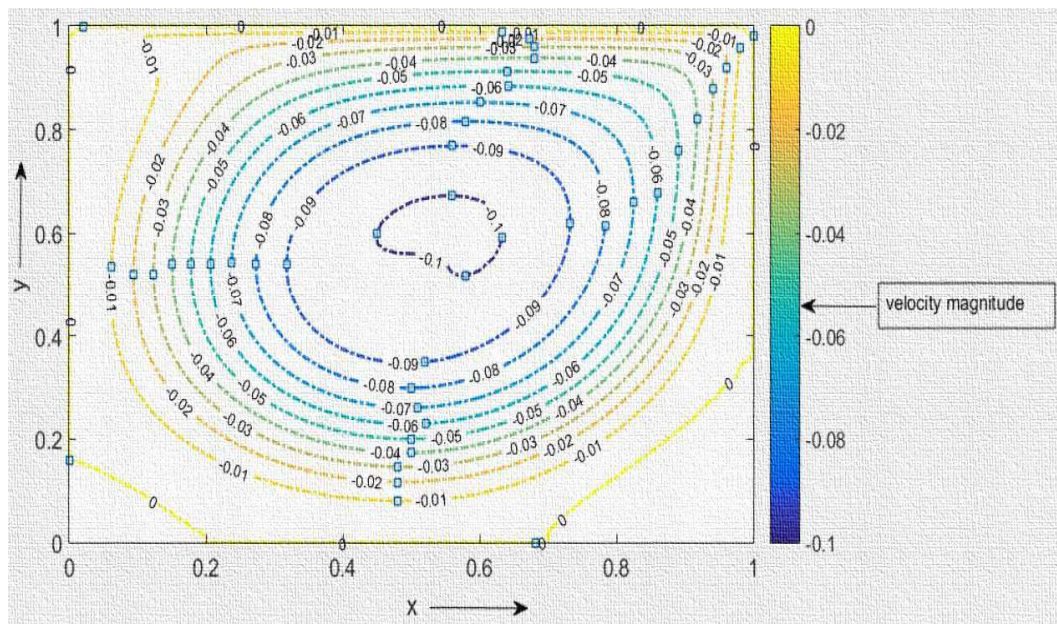


Figure 4. 17 : Stream trajectories of transverse averaged flow component u^y for problem domain (50x50 grid size) at blockage size (0.1 of total length of cavity) and Re=1000

Case-2: With blockage size (0.1 of the total length of lid driven cavity) and reynold number (Re=1000)

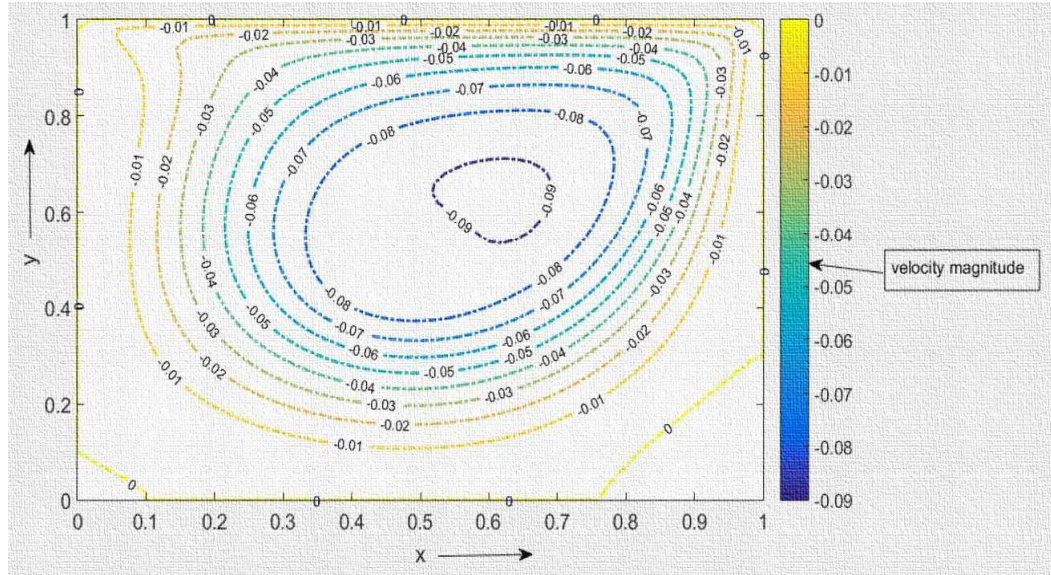


Figure 4. 18 : Stream trajectories of transverse averaged flow component u^y for problem domain (50x50 grid size) at blockage size (0.1 of total length of cavity) at Re=1000

Case-3: With blockage size (0.1 of the total length of lid driven cavity) and reynold number (Re=100)

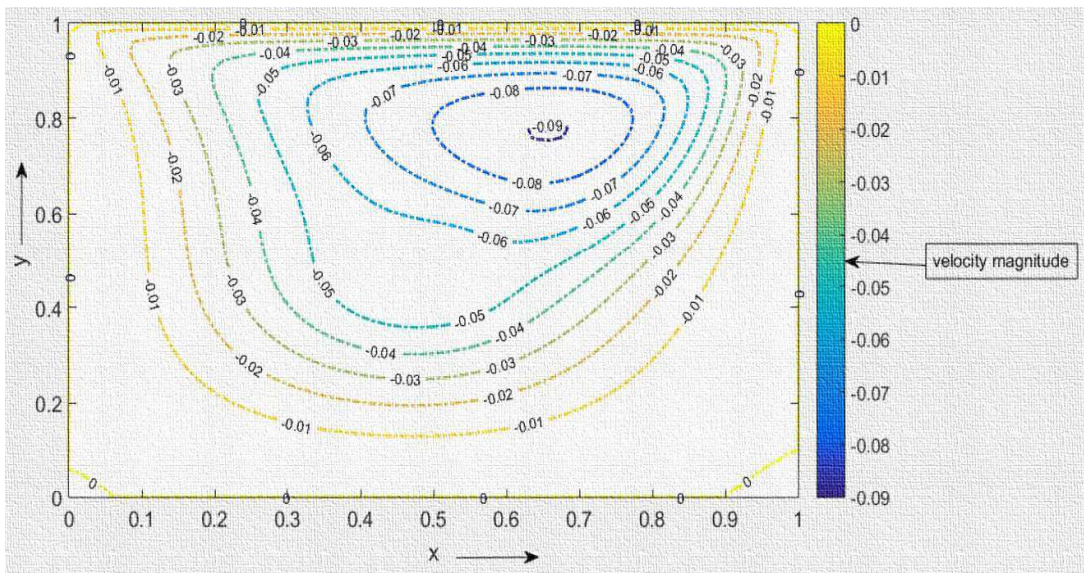


Figure 4. 19 : Stream trajectories of transverse averaged flow component u^y for problem domain (50x50 grid size) at blockage size (0.1 of total length of cavity) and Re=100

Case-4: With blockage size (0.2 of the total length of lid driven cavity) and reynold number (Re=1000)

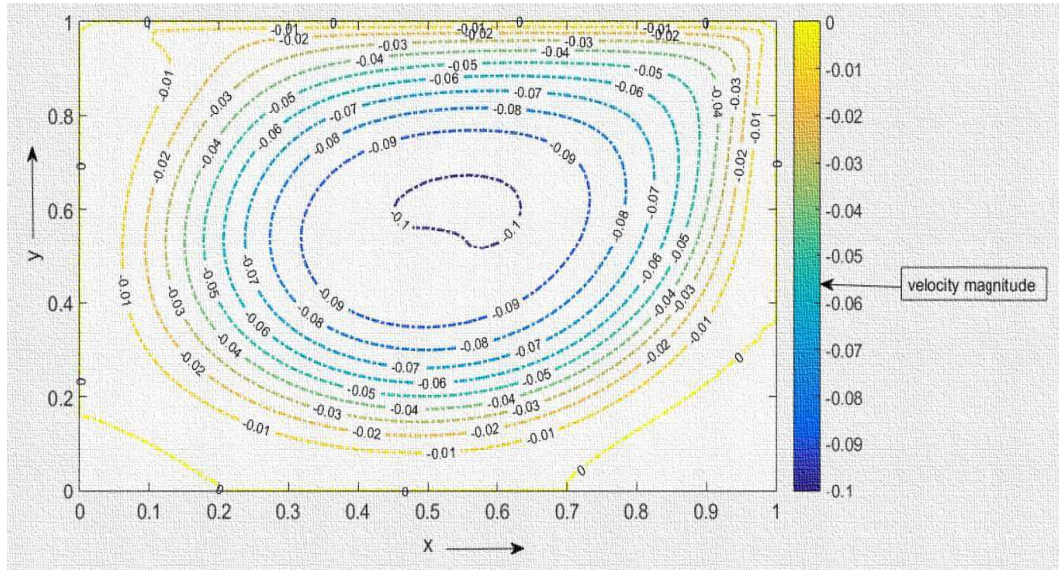


Figure 4. 20 : Stream trajectories of transverse averaged flow component u^y for problem domain (50x50 grid size) at blockage size (0.2 of total length of cavity) and Re=1000

Case-5: With blockage size (0.2 of the total length of lid driven cavity) and reynold number (Re=400)

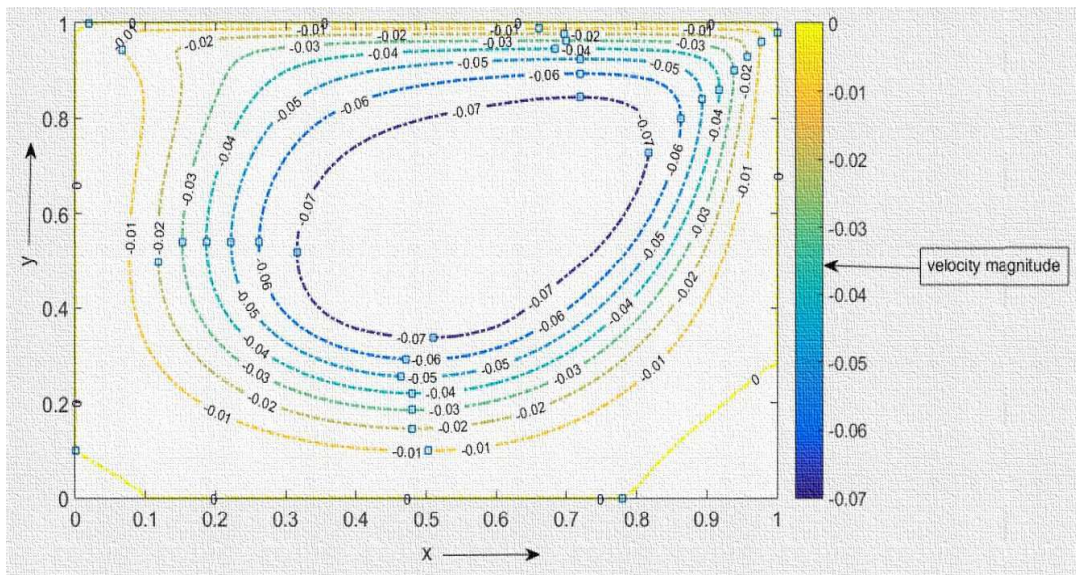


Figure 4. 21 : Stream trajectories of transverse averaged flow component u^y for problem domain (50x50 grid size) at blockage size (0.2 of total length of cavity) and Re=400

Case-6: With blockage size (0.2 of the total length of lid driven cavity) and reynold number (Re=100)

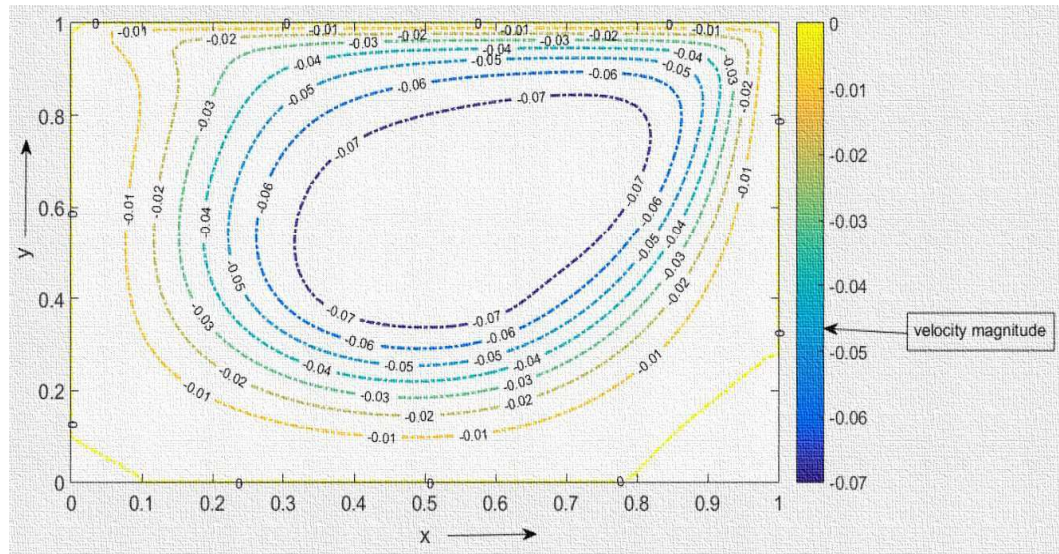


Figure 4. 22 : Stream trajectories of transverse averaged flow component u^y for problem domain (50x50 grid size) at blockage size (0.2 of total length of cavity) and $Re=100$

The above six defined cases show the contours of stream lines of u^y at geometrical vertical centerline of lid driven cavity for 50x50 grid size at blockage sizes (0.1 and 0.2 of total length of cavity) and reynold numbers 1000,400 and 100 respectively. It can be concluded that as there is a decrement in reynold number (from 1000 to 400) for same blockage size, as shown in cases 1 and 2, the velocity peak decrease from 0.1 to 0.09. The similar indication is given by cases 4 and 5.i.e. there is a decrease in velocity magnitude, when there is decrement in Reynolds number from 1000 to 400. But for cases 4 and 5, the given blockage size has been increased from 0.1 to 0.2 of total length of cavity, due to which the fall in velocity peak is more.i.e. from 0.1 to 0.07. As reynold number falls from 400 to 100 for both blockage sizes, as shown in cases (2,3 and 5,6) respectively, there is a very little change or negligible difference noticed in velocity profile of u^y . For the both blockage sizes, it is easily noticeable that as reynold number falls, the vortex core get shifted towards upper side of lid because there is vortex movement there, as it is constantly moving and lower side is observing low or very small velocity.i.e. the flow is more evenly diffused at higher reynold number 1000 and the contours lines are well centered and uniformly distributed over flow domain, as compared with the contours at $Re=400$ and 100, where they are unevenly dispersed and shifting upwards.

CHAPTER 5

CONCLUSIONS AND SCOPE FOR FUTURE WORK

5.1 CONCLUSIONS

1. On increasing number of nodes or decreasing mesh spacing, generally, the error reduces to lower values for any of the described equations for any given method.
2. In case of diffusion and convection dominant diffusion cases, NIM proves to be far ahead in obtaining accurate results as compared to FDM.
3. For coarse mesh sizes, NIM is far better, less tedious and converges to very low errors as compared to FDM.
4. For a lid driven cavity with square blockage at center, the blockage size plays a crucial role in any deviation noticed in velocity profiles at lower reynold numbers.
5. For a lid driven cavity with square blockage at center, the fall observed in velocity peak is more when the blockage size increases for same decrement in reynold number.
6. For a lid driven cavity with square blockage at center, the uniformly dispersed vortex core over flow domain at high reynold number, gets shifted upwards as there is a decrease in reynold number due to high velocity at upper lid because of constant upper lid movement, as compared to low velocity on the lower lid, with decrement in reynold number, irrespective of blockage size.

5.2 SCOPE FOR FUTURE WORK

1. In the created NIM scheme, discretization is finished utilizing ordinary lattices without biasing and non-symmetry of grids consequently in further examinations NIM scheme can be produced for progressively complex areas utilizing one-sided and non-symmetrical frameworks.
2. The linearization of Navier-Stokes conditions is done in present work utilizing focal differencing scheme. SOU (second request upwind) or QUICK (Quadratic Upstream Interpolation for Convective Kinetics) can be utilized for linearization for further investigations.

3. The pressure-velocity coupling is finished utilizing SIMPLE like calculation in the NIM scheme-based plans of Navier-Stokes conditions. Hence increasingly effective methodology for pressure-velocity coupling could be utilized to decrease the computational endeavours of created scheme.
4. In iterating method of present work, Gauss-Siedel solver with Picard linearization is utilized for both linear and non-linear equations. However, this technique has its own conspicuous impediment for non-linear equations. Subsequently for future examinations other effective strategies like JFKM (Jacobian Free Newton Krylov Method) non-linear solver which depends on Newton strategy can be utilized.
5. Likewise, parallel calculation approach as MPI (Message Passing Interface) and multi-framework approach can be utilized in further examinations for growing progressively exact and computational effective solvers dependent on nodal integral strategies.

REFERENCES

1. Uddin, Rizwan. "An improved coarse-mesh nodal integral method for partial differential equations." *Numerical Methods for Partial Differential Equations* 13, no. 2 (1997): 113-145.
2. Fuchs, L., and N. Tillmark. "Numerical and experimental study of driven flow in a polar cavity." *International journal for numerical methods in fluids* 5, no. 4 (1985): 311-329.
3. Azmy, Y. Y. *A nodal integral method for the neutron diffusion equation in cylindrical geometry*. No. CONF-870601-2. Oak Ridge National Lab., TN (USA), 1987.
4. Wang, Fei. "A modified nodal scheme for the time-dependent, incompressible Navier–Stokes equations." *Journal of Computational Physics* 187, no. 1 (2003): 168-196.
5. Fischer, Hans Dieter, and Herbert Finnemann. "The nodal integration method-A diverse solver for neutron diffusion problems." *Atomkernenergie Kerntechnik* 39, no. 4 (1981): 229-236.
6. Azmy, Y. Y. "A nodal integral approach to the numerical solution of partial differential equations." *Proc. Topical Mtg. on Advances in Reactor Computations, Salt Lake City, 1983*(1983).
7. Toreja, Allen J. "Hybrid numerical methods for convection–diffusion problems in arbitrary geometries." *Computers & fluids* 32, no. 6 (2003): 835-872.
8. Azmy, Y. Y. "Nodal methods for problems in fluid mechanics and neutron transport." (1985).
9. Nezami, Erfan G., Suneet Singh, and Nahil Sobh. "A nodal integral method for quadrilateral elements." *International journal for numerical methods in fluids* 61, no. 2 (2009): 144-164.
10. Fitzpatrick, William Edward. "Developments in nodal reactor analysis tools for hexagonal geometry." (1996): 1678-1678.
11. Hu, Yongming, and Xianfeng Zhao. "A nodal green's function method of cylindrical geometry." *Chinese Journal of Nuclear Science and Engineering* 18, no. 3 (1998): 235-243.
12. Kumar, Neeraj, Suneet Singh, and J. B. Doshi. "Pressure Correction–Based Iterative Scheme for Navier-Stokes Equations using Nodal Integral Method." *Numerical Heat Transfer, Part B: Fundamentals* 62, no. 4 (2012): 264-288.
13. Kumar, Neeraj, Suneet Singh, and J. B. Doshi. "Nodal Integral Method Using Quadrilateral Elements for Transport Equations: Part 1—Convection-diffusion Equation." *Numerical Heat Transfer, Part B: Fundamentals* 64, no. 1 (2013): 1-21.

14. Kumar, Neeraj, Suneet Singh, and J. B. Doshi. "Nodal Integral Method Using Quadrilateral Elements for Transport Equations: Part 2-Navier-Stokes Equations." *Numerical Heat Transfer, Part B: Fundamentals* 64, no. 1 (2013): 22-47.
15. Komlev, O. G., and I. R. Suslov. "A nodal expansion method for the neutron diffusion equation in cylindrical geometry." In *Proceedings of the international conference on mathematics and computations, reactor physics, and environmental analyses. Volume 1 and 2*. 1995.
16. Kim, Sung T., and J. J. Doming. "Discrete Nodal and Sn Transport Methods for Irregularly Shaped Shields." *Nuclear Science and Engineering* 105, no. 1 (1990): 16-30.
17. Lawrence, Richard Douglas, and J. J. Dorning. "A nodal Green's function method for multidimensional neutron diffusion calculations." *Nuclear Science and Engineering* 76, no. 2 (1980): 218-231.
18. Azmy, Y. Y. "A nodal integral approach to the numerical solution of partial differential equations." *Proc. Topical Mtg. on Advances in Reactor Computations, Salt Lake City, 1983*(1983).
19. Horak, W. C., and J. J. Dorning. "A nodal coarse-mesh method for the efficient numerical solution of laminar flow problems." *Journal of Computational Physics* 59, no. 3 (1985): 405-440.
20. Hennart, Jean Pierre. "On the numerical analysis of analytical nodal methods." *Numerical methods for partial differential equations* 4, no. 3 (1988): 233-254.
21. Wilson, G. L., R. A. Rydin, and Y. Y. Azmy. "A time-dependent nodal-integral method for the investigation of bifurcation and nonlinear phenomena in fluid flow and natural convection." *Nuclear Science and Engineering* 100, no. 4 (1988): 414-425.
22. Michael, E. P. E., J. Dorning, and Rizwan-Uddin. "Studies on nodal integral methods for the convection-diffusion equation." *Nuclear science and engineering* 137, no. 3 (2001): 380-399.
23. Uddin, Rizwan. "A second-order space and time nodal method for the one-dimensional convection-diffusion equation." *Computers and Fluids* 26, no. 3 (1997): 233-247.
24. Uddin, Rizwan. "An improved coarse-mesh nodal integral method for partial differential equations." *Numerical Methods for Partial Differential Equations* 13, no. 2 (1997): 113-145.
25. Huang, Kai, and U. Rizwan. "Modified nodal integral method incorporated with irregular-shape elements for Navier-Stokes equations." (2009).

26. Burns, T. J., and J. J. Dorning. *Partial current balance method: a new computational method for the solution of multidimensional neutron diffusion problems*. No. MRR-145; CONF-750134-. Oak Ridge National Lab., TN; Technische Univ. Muenchen, Garching (FR Germany). Lab. fuer Reaktorregelung und Anlagensicherung, 1975.
27. Ollivier-Gooch, Carl, and Michael Van Altena. "A high-order-accurate unstructured mesh finite volume scheme for the advection–diffusion equation." *Journal of Computational Physics* 181, no. 2 (2002): 729-752.
28. Saidi, Maysam, Hassan Basirat Tabrizi, and Reza Maddahian. "Vortex Formation in Lid-driven Cavity with Disturbance Block." *World Academy of Science, Engineering and Technology, International Journal of Mathematical, Computational, Physical, Electrical and Computer Engineering* 6, no. 9 (2012): 1356-1359.
29. Kosti, Siddhartha, and Vaibhav S. Rathore. "Numerical Study of Lid Driven Cavity at Different Reynolds Number." *Trends in Mechanical Engineering & Technology (TMET)* 5, no. 3 (2015): 1-5p.
30. Peng, Yih-Ferng, Yuo-Hsien Shiau, and Robert R. Hwang. "Transition in a 2-D lid-driven cavity flow." *Computers & Fluids* 32, no. 3 (2003): 337-352.

APPENDIX

Coefficients of discrete Eqs. (3.25 to 3.30) are as follows:

$$F_{11} = \left\{ \frac{1}{2b} - \frac{3b}{2(a^2+b^2)} \right\}_{i,j+1} \quad (A.1)$$

$$F_{13} = \left\{ \frac{1}{2b} - \frac{3b}{2(a^2+b^2)} \right\}_{i,j} \quad (A.2)$$

$$F_{12} = \left[\left\{ \frac{1}{2b} + \frac{3b}{2(a^2+b^2)} \right\}_{i,j} + \left\{ \frac{1}{2b} + \frac{3b}{2(a^2+b^2)} \right\}_{i,j+1} \right] \quad (A.3)$$

$$F_{14} = \left\{ \frac{3b}{2(a^2+b^2)} \right\}_{i,j} \quad (A.4)$$

$$F_{15} = \left\{ \frac{3b}{2(a^2+b^2)} \right\}_{i,j+1} \quad (A.5)$$

$$F_{16} = - \left\{ \frac{\rho a^2 b}{(a^2+b^2)} \right\}_{i,j} \quad (A.6)$$

$$F_{17} = - \left\{ \frac{\rho a^2 b}{(a^2+b^2)} \right\}_{i,j} \quad (A.7)$$

Since coefficients for discrete pressure equations are geometry dependent thus F_{21} to F_{27} could be reproduce from Eqs. (A.1) to (A.7) by replacing a by b and i by j . Coefficients for discretize momentum Eq. (2.52) are

$$F_{31} = \left[\frac{1}{2b} \left\{ \frac{pev}{e^{pev}-1} \right\} + \frac{2b}{v} \left\{ \frac{1}{e^{pev}-1} - \frac{1}{pev} \right\} \frac{1}{A} \left\{ \frac{1}{pev} - \frac{1}{e^{pev}-1} \right\} \right]_{i,j+1} \quad (A.8)$$

$$F_{33} = \left[\frac{1}{2b} \left\{ \frac{pev}{1-e^{-pev}} \right\} + \frac{2b}{v} \left\{ \frac{1}{1-e^{-pev}} - \frac{1}{pev} \right\} \frac{1}{A} \left\{ \frac{1}{pev} - \frac{1}{1-e^{-pev}} \right\} \right]_{i,j} \quad (A.9)$$

$$F_{32} = \left[\frac{1}{2b} \left\{ \frac{pev}{e^{pev}-1} \right\} + \frac{2b}{v} \left\{ \frac{1}{e^{pev}-1} - \frac{1}{pev} \right\} \frac{1}{A} \left\{ \frac{1}{pev} - \frac{1}{1-e^{-pev}} \right\} \right]_{i,j+1} + \left[\frac{1}{2b} \left\{ \frac{pev}{1-e^{-pev}} \right\} + \frac{2b}{v} \left\{ \frac{1}{1-e^{-pev}} - \frac{1}{pev} \right\} \frac{1}{A} \left\{ \frac{1}{pev} - \frac{1}{e^{pev}-1} \right\} \right]_{i,j} \quad (A.10)$$

$$F_{34} = \left[\frac{2b}{v} \left\{ \frac{1}{1-e^{-pev}} - \frac{1}{pev} \right\} \frac{1}{A} \left\{ \frac{1}{1-e^{-peu}} - \frac{1}{peu} \right\} \right] \quad (A.11)$$

$$F_{35} = \left[\frac{2b}{v} \left\{ \frac{1}{1-e^{-pev}} - \frac{1}{pev} \right\} \frac{1}{A} \left\{ \frac{1}{peu} - \frac{1}{e^{peu}-1} \right\} \right] \quad (A.12)$$

$$F_{36} = \left[\frac{2b}{v} \left\{ \frac{1}{e^{pev}-1} - \frac{1}{pev} \right\} \frac{1}{A} \left\{ \frac{1}{1-e^{-peu}} - \frac{1}{peu} \right\} \right] \quad (A.13)$$

$$F_{37} = \left[\frac{2b}{v} \left\{ \frac{1}{e^{pev}-1} - \frac{1}{pev} \right\} \frac{1}{A} \left\{ \frac{1}{peu} - \frac{1}{e^{peu}-1} \right\} \right] \quad (A.14)$$

$$F_{38} = \left[\frac{2b}{v} \left\{ \frac{1}{1-e^{-pev}} - \frac{1}{pev} \right\} \frac{1}{A} E \right]_{i,j} \quad (A.15)$$

$$F_{39} = \left[\frac{2b}{v} \left\{ \frac{1}{e^{pev}-1} - \frac{1}{pev} \right\} \frac{1}{A} E \right]_{i,j+1} \quad (A.16)$$

where

$$A = \left[\frac{2a^2}{v} \left\{ \frac{1}{peu} \left(\frac{e^{peu}+1}{e^{peu}-1} \right) - \frac{2}{peu^2} \right\} + \frac{2b^2}{v} \left\{ \frac{1}{Rev} \left(\frac{e^{pev}+1}{e^{pev}-1} \right) - \frac{2}{pev^2} \right\} \right] \quad (A.17)$$

$$E = \frac{2a^2}{v} \left\{ \frac{1}{peu} \left(\frac{e^{peu}+1}{e^{peu}-1} \right) - \frac{2}{peu^2} \right\} \quad (A.18)$$

Since the formulation is of symmetric in nature thus the expression for coefficient from F_{41} to F_{49} could be generated by replacing a by b, peu by pev , i by j and its vica-versa.

The limiting values of the exponential expression could be express by Taylor expansion,

$$\lim_{x \rightarrow 0} \frac{x}{e^x-1} = 1 - \frac{x}{2} + \frac{x^2}{12} + \dots \quad (A.19)$$

$$\lim_{x \rightarrow 0} \frac{x}{1-e^{-x}} = 1 + \frac{x}{2} + \frac{x^2}{12} + \dots \quad (A.20)$$

$$\lim_{x \rightarrow 0} \frac{1}{e^x-1} = -\frac{1}{2} + \frac{1}{x} + \frac{x}{12} + \frac{x^3}{720} + \dots \quad (A.21)$$

$$\lim_{x \rightarrow 0} \frac{1}{1-e^{-x}} = \frac{1}{2} + \frac{1}{x} + \frac{x}{12} - \frac{x^3}{720} + \dots \quad (A.22)$$

$$\lim_{x \rightarrow 0} \frac{e^x+1}{e^x-1} = \frac{2}{x} + \frac{x}{6} - \frac{x^3}{360} + \dots \quad (A.23)$$

Coefficients of discrete Eqs.(3.12 and 3.13) are as follows:

$$A = \frac{k}{2 \times a \times u} - E \quad (\text{A.24})$$

$$X = \frac{1}{k} \left\{ \frac{1}{\left(\frac{u}{k}\right)^2} - \frac{k \times a}{u} - \frac{2 \times k \times a \times E}{u} \right\} \quad (\text{A.25})$$

$$B = 1 - A \quad (\text{A.26})$$

$$D = 2 \times a \times F - \frac{\alpha}{u} \quad (\text{A.27})$$

$$E = \frac{1}{e^{\frac{2 \times a \times u}{\alpha}} - 1} \quad (\text{A.28})$$

$$F = \frac{1}{1 - e^{-\frac{2 \times a \times u}{\alpha}}} \quad (\text{A.29})$$

$$G = \frac{D}{2 \times b} \quad (\text{A.30})$$

Turnitin Originality Report

Processed on: 19-Jul-2019 16:15 +0530

ID: 978682810

Word Count: 12003

Submitted: 4

APPLICATION OF NODAL INTEGRAL METHOD FOR CONVECTION-DIFFUSION

PHYSICS AND NAVIER-STOKES
EQUATIONS By Neeraj Kumar

1% match (publications)

[Neeraj Kumar, Suneet Singh, J. B. Doshi.](#)

["Pressure Correction-Based Iterative Scheme for Navier-Stokes Equations using Nodal Integral Method", Numerical Heat Transfer, Part B: Fundamentals, 2012](#)

Similarity Index	Similarity by Source	
11%	Internet Sources:	5%
	Publications:	7%
	Student Papers:	6%

1% match (publications)

[Rishabh Prakash Sharma,](#)

[Neeraj Kumar. "Nodal integral method for convection-diffusion transport using linear and higher order quadrilateral elements", Numerical Heat Transfer, Part B: Fundamentals, 2018](#)

1% match (Internet from 07-Nov-2018)

https://personalpages.manchester.ac.uk/staff/david.silvester/ESW2005_ch3ex.pdf

1% match (publications)

[Rizwan-uddin. "An improved coarse-mesh nodal integral method for partial differential equations", Numerical Methods for Partial Differential Equations, 03/1997](#)

< 1% match (publications)

[Xu, M.. "A discrete particle model for particle-fluid flow with considerations of sub-grid structures", Chemical Engineering Science, 200704](#)

< 1% match (publications)

[Chunxiao Liu. "Distortion Optimization based Image Completion from a Large Displacement View", Computer Graphics Forum, 10/2008](#)

< 1% match (student papers from 28-Jun-2018)

[Submitted to Indian Institute of Science Education and Research on 2018-06-28](#)

< 1% match (student papers from 11-Jul-2018)

[Submitted to Indian Institute of Technology, Bombay on 2018-07-11](#)

< 1% match (student papers from 06-Mar-2011)

[Submitted to National University of Singapore on 2011-03-06](#)

< 1% match (Internet from 01-May-2019)

http://epubs.surrey.ac.uk/842258/1/PhD%20Thesis_Wei%20Liu_12_Sep.pdf

< 1% match (publications)

[D. Senthil Kumar. "Numerical Simulation of Double Diffusive Mixed Convection in a Lid-Driven Square Cavity Using Velocity-Vorticity Formulation", Numerical Heat Transfer Part A Applications, 01/2008](#)

< 1% match (Internet from 27-Apr-2010)

<http://www.answers.com/topic/stream-function>

< 1% match (student papers from 29-Jun-2018)

[Submitted to Thapar University, Patiala on 2018-06-29](#)

< 1% match (publications)

[Erfan G. Nezami. "A nodal integral method for quadrilateral elements", International Journal for Numerical Methods in Fluids, 2008](#)

< 1% match (student papers from 14-Jul-2016)

[Submitted to Thapar University, Patiala on 2016-07-14](#)

< 1% match (Internet from 26-Sep-2014)

<http://turhancoban.com/kitap/NUMERICAL%20HEAT%20CONDUCTION.htm>

< 1% match (Internet from 26-Sep-2017)

<https://researchonline.jcu.edu.au/49460/1/49460-Inam-2016-thesis.pdf>

< 1% match (student papers from 06-Mar-2013)

[Submitted to Middle East Technical University on 2013-03-06](#)

< 1% match (Internet from 09-Apr-2010)

<http://www.coursehero.com/file/279761/ELmethod/>

< 1% match (Internet from 06-Dec-2016)

<https://digital.library.adelaide.edu.au/dspace/bitstream/2440/66344/9/01front.pdf>

< 1% match (publications)

[Trangenstein, J.A.. "Multi-scale iterative techniques and adaptive mesh refinement for flow in porous media", Advances in Water Resources, 200208/12](#)

< 1% match (publications)

[R.D. Lawrence. "Progress in nodal methods for the solution of the neutron diffusion and transport equations", Progress in Nuclear Energy, 1986](#)

< 1% match (student papers from 15-Mar-2018)

[Submitted to High School Attached to Northeast Normal University on 2018-03-15](#)

< 1% match (Internet from 29-Nov-2018)

<https://es.scribd.com/document/62333464/DESIGN-DEVELOPMENT-OF-A-PYROLYSIS-REACTOR>

< 1% match (publications)

[Suneet Singh, Rizwan-uddin. "k-ε modeling using modified nodal integral method", Nuclear Engineering and Design, 2009](#)

< 1% match (Internet from 29-Apr-2019)

<http://etheses.whiterose.ac.uk/15223/1/549721.pdf>

< 1% match (student papers from 16-Jan-2017)

[Submitted to Universiti Sains Malaysia on 2017-01-16](#)

< 1% match (publications)

[Kim, Chongam. "Multi-Dimensional Limiting Process for Flow Physics Analyses on Structured and Unstructured Grids", COMPUTATIONAL FLUID DYNAMICS REVIEW 2010, 2010.](#)

< 1% match (student papers from 04-May-2016)

[Submitted to Cardiff University on 2016-05-04](#)

< 1% match (student papers from 07-May-2015)

[Submitted to University of Sheffield on 2015-05-07](#)

< 1% match (Internet from 25-Sep-2010)

<http://pefmath.etf.rs/vol4num1/AADM-Vol4-No1-136-155.pdf>

< 1% match (publications)

[Advances in Geophysical and Environmental Mechanics and Mathematics, 2014.](#)

< 1% match (student papers from 24-May-2016)
[Submitted to Indian Institute of Information Technology, Design and Manufacturing - Kancheepuram on 2016-05-24](#)

< 1% match (student papers from 05-Sep-2016)
[Submitted to Imperial College of Science, Technology and Medicine on 2016-09-05](#)

< 1% match (Internet from 09-Mar-2016)
<http://ethesis.nitrkl.ac.in/6394/1/E-9.pdf>

< 1% match (Internet from 16-Jul-2019)
<https://en.wikipedia.org/wiki/Streamfunction>

< 1% match (Internet from 15-May-2016)
<https://www.deepdyve.com/browse/journals/computers-and-fluids/2003/v32/i6>

< 1% match (student papers from 04-Jul-2019)
[Submitted to Thapar University, Patiala on 2019-07-04](#)

< 1% match (student papers from 15-Apr-2019)
[Submitted to Delhi University on 2019-04-15](#)

< 1% match (Internet from 17-Apr-2019)
<https://pastel.archives-ouvertes.fr/tel-01885220/document>

< 1% match (Internet from 09-Mar-2016)
<http://ethesis.nitrkl.ac.in/6392/1/E-11.pdf>

< 1% match (Internet from 27-May-2019)
http://jafmonline.net/JournalArchive/download?file_ID=46631&issue_ID=250

< 1% match (Internet from 16-Apr-2016)
<https://ira.le.ac.uk/bitstream/2381/10941/1/2012packwooddphd.pdf>

< 1% match (publications)
[Niteen Kumar, Rudrodip Majumdar, Suneet Singh. "Physics-based preconditioning of Jacobian free Newton Krylov for Burgers' equation using modified nodal integral method", Progress in Nuclear Energy, 2019](#)

< 1% match (student papers from 05-Apr-2013)
[Submitted to Indian Institute of Technology, Bombay on 2013-04-05](#)

< 1% match (student papers from 28-Jan-2011)
[Submitted to Higher Education Commission Pakistan on 2011-01-28](#)

< 1% match (student papers from 20-May-2019)
[Submitted to Institut Teknologi Brunei on 2019-05-20](#)

< 1% match (Internet from 26-Dec-2017)
<https://d-nb.info/1122740964/34>

< 1% match (Internet from 17-Feb-2019)
https://baadalsg.inflibnet.ac.in/bitstream/10603/134639/11/11_chapter%205.pdf

< 1% match (Internet from 07-Mar-2016)
<http://www.ans.org/store/article-19452/>

< 1% match (publications)
[Pengfei Wang, Rizwan-uddin. "A modified, hybrid nodal-integral/finite-element method for 3D convection-diffusion problems in arbitrary geometries", International Journal of Heat and Mass Transfer, 2018](#)

< 1% match (publications)

< 1% match (student papers from 19-Jan-2018)

[Submitted to Savitribai Phule Pune University on 2018-01-19](#)

APPLICATION OF NODAL INTEGRAL METHOD FOR CONVECTION-DIFFUSION PHYSICS AND NAVIER-STOKES EQUATIONS [THESIS SUBMITTED IN PARTIAL FULFILLMENT OF REQUIREMENTS FOR THE DEGREE OF MASTER OF ENGINEERING IN THERMAL ENGINEERING BY YUVRAJ SINGH REGISTRATION NO.: 801783018 UNDER THE SUPERVISION OF DR. NEERAJ KUMAR \(ASSISTANT PROFESSOR\), MECHANICAL ENGINEERING DEPARTMENT THAPAR INSTITUTE OF ENGINEERING AND TECHNOLOGY, PATIALA- 147004, PUNJAB, INDIA](#) CERTIFICATE I hereby declare [that the](#) dissertation entitled "APPLICATION OF NODAL INTEGRAL METHOD FOR CONVECTION-DIFFUSION PHYSICS AND NAVIER-STOKES EQUATIONS" [is an authentic record of my work carried out as requirements for the award of the degree of](#) Master [of](#) Engineering [in](#) Thermal Engineering [at Thapar Institute of Engineering and Technology, Patiala under the supervision of Dr. Neeraj Kumar \(Assistant Professor, Mechanical Engineering Department\)](#). [No part of the matter embodied in this report has been submitted to any other university or institute for the award of any degree.](#) Date: 17-July-2019 Yuvraj Singh Roll No.801783018 Thapar Institute of Engineering and Technology, Patiala [It is certified that the above statement made by the student is correct to the best of my knowledge and belief.](#) Dr. Neeraj Kumar [Assistant Professor Mechanical Engineering Department Thapar Institute of Engineering and Technology,](#) Patiala i [ABSTRACT Generic nodal integral method \(NIM\) based scheme](#) is being utilized [to solve](#) the [diffusion,](#) convection-[diffusion](#) problems [and navier-stokes equations in](#) regular rectangle cartesian geometry. The problems taken into account in present work are 2D steady state diffusion with heat source, 1D steady state diffusion, 2D steady state convection-diffusion with heat source and flow in lid driven cavity with square obstacle at center. Numerical results for FDM and NIM [are compared, with](#) respect to [analytical solution for diffusion and convection -diffusion](#) problems. Different respective grid sizes have been used to capture problem flow domain for diffusion, convection-diffusion and lid driven cavity. The flow in lid driven cavity with square obstacle at center has been modelled successfully using discretized navier-stokes equations utilizing NIM. In case of diffusion and convection dominant diffusion, the NIM scheme yields far better results as compared to FDM for any given grid size and takes less computational time as contrasted with latter. For coarser meshes specifically, for most of the defined cases, the NIM converges to very low errors in comparison to FDM.i.e. approximately ten to hundred times less than latter. Due to this reason, in the present work, the NIM modelled discretized navier stokes equations has been used effectively to capture the flow profiles efficiently for lid driven cavity at any grid size, coarser or finer, for high or low reynold numbers ranging from 100 to 1000. ii ACKNOWLEDGEMENTS [I would like to express my special thanks and sense of gratitude to my supervisor, Dr. Neeraj Kumar for the guidance. I have been extremely lucky to have a supervisor who helped me in my work and I came to know about so many new things. He provided me the technical support, facilities and skills that really helped me during the work. He cared so much about my work over the year. Furthermore, I would like to express my sincere gratitude to the Mechanical Engineering Department, Thapar Institute of Engineering and Technology for the technical support. Further, I would like to thank specially my lab. members Amritpal Singh, Sandeep Nain and Gurmeet Singh for their technical and moral support. Finally, I would like to express my sincerest sense of gratitude to my family for their support and love for me, without which this work could not have been possible.](#) iii TABLE OF CONTENTS Page No. Certificate i Abstract ii Acknowledgements iii Table of Contents iv List of Figures v List of Tables vii Nomenclature viii Abbreviations ix CHAPTER 1 INTRODUCTION 1 1.1 Motivation 1 1.2 Thesis Outline 3 CHAPTER 2 LITERATURE REVIEW 4 2.1 Introduction 4 2.2 Notable work 5 2.3 Gaps identified 11 2. 4 Thesis objectives 12 CHAPTER 3 MATHEMATICAL FORMULATION 13 3.1 Basic methodology 13 3.2 Discretized steady state 2D equation with heat source 17 3.3 Discretized 1D convection-diffusion equation 18 3.4 Discretized steady state 2D convection-diffusion equation with 18 heat source 3.5 Discretized Navier Stokes Equations 19 CHAPTER 4 NUMERICAL